

# CHARACTERISTICS AND APPLICATIONS OF MICROSTRIP FOR MICROWAVE WIRING

M. Arditi  
Federal Telecommunication Laboratories  
Division of International Telephone and Telegraph Corporation  
Nutley, New Jersey

## Introduction

Microstrip<sup>2,3,4</sup> has been developed as a substitute for waveguides or coaxial lines, especially for the development of microwave components and Microwave circuitry.<sup>5</sup>

Microstrip is a wide-band transmission system in which the electromagnetic waves are propagated through a dielectric medium bonded by a strip conductor on one side and a conducting ground plane on the other side, the distance between the strip conductor on the ground plane being a small fraction of the wavelength of the line. With this type of line, the manufacture of microwave plumbing reduces itself to a printed circuit technique, susceptible of great accuracy, adaptable to mass production, and resulting in great savings in cost, space, and weight.

In addition to Microstrip, various types of strip-lines have been known for some time<sup>1,6,7,8</sup> (see Fig. 1). Except for Microstrip, most of these structures are equivalent to flat coaxial lines, with or without dielectric filling. With the structure shown in Fig. 1C, it is possible to obtain high Q's because the conductor losses are the only important ones; therefore this type of line permits the design of high Q components, such as microwave filters.<sup>6</sup> Due to the losses in the line, particularly the dielectric losses, Microstrip, in its usual form, may not always be suitable for long transmission lines or high Q filters. As will be shown later, the losses in the line are more comparable to the losses obtained with dielectric-filled coaxial lines than to the losses in air-filled waveguides. However, there are many microwave circuits and microwave components where high Q quality is not essential, and it is in these circuits where Microstrip may prove more practical or more economical than cylindrical or flat coaxial structures. It is easy to couple external high Q cavities or filters to Microstrip, and the resulting radiation from the low Q line, being small, simplifies the shielding problem.

Thus, in general, a Microstrip circuit will be designed having low Q lines for most of its parts, and with the

coaxial standing-wave machine. The length of the Microstrip is varied, over half a insertion of a few external high Q components. Very often this combination will result in a simplification of the system, or in some economical advantages.

Fig. 2 shows various Microstrip lines and components and, for comparison, some low-frequency printed circuits. The same etching or engraving processes can be utilized, and sometimes both types of circuits will be printed on the same board at the same time (see Fig. 3).

Before discussing the transmission properties of Microstrip and the characteristics of various Microstrip components, the method of measurement used with Microstrip will be described briefly.

## Technique of Measurements in Microstrip

Since the geometry of Microstrip is rather unconventional, the usual measurement technique in microwaves must be modified to obtain the characteristics of the line, i.e., phase velocity and attenuation, or the characteristics of obstacles in the line. For example, a probe can be used only to obtain information on the field distribution in a region far from the main power flow. Also, a probe inserted in a slot in the ground plane under the strip conductor will alter the normal mode of propagation of the microwave energy flowing along the line. For the above reasons, it has been found convenient to make all impedance measurements on Microstrip by connecting this line, through a transducer, to an ordinary waveguide or coaxial slotted line. The reflections from the Microstrip line are then measured in the standard manner.

Although the method has been described originally by G. Deschamps<sup>9</sup> for the determination of the reflections coefficients and attenuation loss of a closed waveguide junction, its application to Microstrip is justified as long as the main power flow along the line is confined in one dominant mode. In general, this has been found to be true.

The experimental set-up is shown in Fig. 4. The Microstrip specimen is connected to an ordinary waveguide or

wavelength, either by moving a short-circuit across the conductors, or by cutting the line at its end. The corresponding reflection coefficient is measured at the input in the standard manner. The successive positions of the short-circuit are arranged to differ by  $\lambda/8$ . When plotted on the complex plane, these reflection coefficients fall on a circle, assuming the losses in the line are small within half a wavelength. The chords joining opposite points intersect in a point that is related in a simple manner to the reflection and transmission coefficient of the junction.

From the circle diagrams, the wavelength or phase velocity of the dominant mode can be easily obtained.

By repeating the measurements for two different lengths of the line with the same junction, the losses in the line per unit length can be obtained.

The use of a "hyperbolic protractor," also developed by G. Deschamps,<sup>9</sup> reduces the computations to mere readings of "hyperbolic distances." (Fig. 6)

A good short-circuit between the conductors is obtained by soldering a large conductor plate between the strip conductor and the ground plane. This method, however, destroys the Microstrip sample and there is no possibility of checking back on the measurements. It is possible to obtain the circle diagram corresponding to the displacement of a good short-circuit without having to cut continuously the end of the line. The experimental set-up is shown in Fig. 5. To this end, the reflection coefficient given by a good short-circuit for only one position in the line is compared with the circle diagram obtained by moving a constant reflective load around this position. A simple geometrical construction can then be applied to obtain the desired results.<sup>9,5</sup>

Deschamps' method permits the determination of the reflection coefficient and insertion loss of the junction between Microstrip and coaxial or waveguide lines. The method also permits the characteristics for any obstacle in Microstrip to be expressed in terms of the scattering matrix coefficients. For example, when measuring a discontinuity, junction A, between two Microstrip lines, through another discontinuity, junction B, (see Fig. 7) one must consider first AB in cascade as a two port linear network, then disconnect junction A and measure the two port network B. From these two measurements, the characteristics of the discontinuity A can be deduced.<sup>9</sup>

### Transmission Properties of Microstrip

An exact theory of this open line has been outlined by G. Deschamps of Federal Telecommunication Laboratories,<sup>9</sup> and M. Schetzen of M.I.T.<sup>10</sup> However, the theory has not yet been reduced to practical formulas. An approximate theory based on the assumption of T.E.M. mode of propagation has been given by F. Assadourian and E. Rimai and published in the PROCEEDINGS of the I.R.E.<sup>3</sup> This theory can be used with good approximation to obtain the values of the principal characteristics of the line.

A T.E.M. mode can propagate in Microstrip only if one considers a lossless system with a uniform dielectric infinite in extent. However, practical Microstrip lines involve a solid dielectric upon which a strip is printed, and an air region above the dielectric. Since Microstrip lines involve composite dielectric and losses, they cannot support a pure T.E.M. mode. Nevertheless, both theory and experiment indicate that the field and power flow are concentrated in the dielectric between the conductors, and that the assumption of a single, infinite dielectric leads to useful results even though it is not rigorous. Fig. 8 shows the theoretical distribution of power flow for a wide strip of zero thickness above an infinite ground plane.<sup>3</sup>

The measured characteristics of the line will now be compared with the results of the first order theory.

### Phase Constant

1. As in a T.E.M. mode of propagation, and over a wide range of frequencies, the phase velocity,  $v$ , is constant to within experimental errors which are less than 0.5%; i.e., Microstrip is not dispersive.

2. In general, the wavelength in Microstrip is longer than the value corresponding to a T.E.M. mode of propagation between infinite parallel plates immersed in a teflon dielectric. For a given thickness of dielectric the wavelength decreases as the width of the strip conductor increases, approaching asymptotically the value of  $\lambda_{TEM}$  for very wide strips (see Fig. 9).

3. To a first approximation, a characteristic impedance can be defined as

$$Z_0 = \frac{1}{Cv}$$

where  $C$  is the measured electrostatic capacitance per unit length, and  $v$  is the measured phase velocity along Microstrip.

The characteristic impedance is a function of the width of the strip line,  $b$ , and the dielectric thickness,  $h$  (see Fig. 10). For purpose of comparison with the theory, Fig. 11 shows the ratio of  $Z_0/Z_0'$  plotted versus  $b/h$ . ( $Z_0'$  corresponds to a constant field in the absence of fringing and leakage flux:

$$Z_0' = \frac{h}{b} \sqrt{\frac{\mu}{\epsilon}}.$$

It can be seen that the agreement with the first order theory is quite good.

### Attenuation Constant

In Microstrip, the attenuation is due to conductor loss, dielectric loss, and radiation loss. The method of measurement gives only the total attenuation. The circle diagram method is used to measure the attenuation along the line for the purpose of studying its uniformity (see Figs. 12 and 13). The attenuation along Microstrip is constant with the exception of a region near the transducer. Fig. 14 shows the variations of the average attenuation over the frequency range from 4000 to 9000 mc for a particular Microstrip line. On the same graph are plotted theoretical attenuation curves obtained from the first order theory assuming a constant loss angle for the dielectric over the entire frequency range. Curve I is the experimentally determined curve; Curve II is a computed curve for a line identical to the experimental model; and Curve III is a computed curve for a similar line but with a dielectric thickness twice as great. The agreement between Curves I and II could be even better if we had assumed, as more probable, that the loss angle increases with frequency.

The average attenuation and unloaded  $Q_0$  of a line 1/16-inch thick are shown in Fig. 15 ( $Q_0 = \pi/\lambda\alpha$ ). For a 1/8-inch-thick line, the average value of attenuation of 1.1 decibels per meter is made up of about 0.3 db/m for the conductor loss and 0.8 db/m for the dielectric loss at 6000 mc. This line corresponds to a  $Q_0$  of about 700 at 6000 mc. By removing the dielectric, the conductor losses are reduced to 0.18db/m with the same geometry, corresponding to a  $Q_0$  of about 3000. Fig. 16 shows a comparison between the attenuation of waveguide, coaxial, and Microstrip lines.

### Power-Handling Capacity

The power-handling capacity of the Microstrip line, like any other dielectric-filled transmission line, is limited by breakdown and dielectric heating.

Usually for CW operation, dielectric

heating will be the limiting factor. Breakdown will be more serious for high-power pulse operation.

For a Microstrip with a line 7/32-inch wide on a base of Teflon impregnated Fiberglas 1/16-inch thick, at 3000 mc with a CW power of 300 watts, the rise in temperature under the strip line was 50°C above the ambient (20°C).

Under pulse conditions, corona effects appear at the edge of the strip conductor for a pulse power around 15 kw at 9000 mc. However, gradients are higher at transducers, and there is a greater possibility of breakdown at these points than in the line. Further measurements must be made before any absolute values of breakdown and corona effects can be given. Special precautions should be taken to round off all sharp edges for pulse operation, and it may be desirable to paint the edges of the strip conductor with a dielectric paint to increase the breakdown voltage.

### Characteristics of Microstrip Components

#### Transducers from Microstrip to Coaxial or Waveguide Lines

Coaxial and Microstrip lines are wide-band transmission systems, and a wide-band transducer between the two lines is a useful item for many Microstrip components.

A standard UG-58/U type N coaxial connector is used to excite the Microstrip line. This type of connector can be utilized over a wide band of frequencies, and is matched to a 50-ohm coaxial line. The connector is mounted at right angle to the plane of the Microstrip line (see Fig. 17). Matching is achieved by employing an iris of proper diameter located in the ground plane. Fig. 18 shows the frequency range of matching, and Fig. 19 shows the total insertion loss in the transducer. This loss is relatively small over a wide frequency band,

By removing the dielectric around the center pin of the transducer, the frequency range of matching can be extended up to 10,000 mc with an insertion loss smaller than 0.6 db (Fig. 20). When smaller insertion loss is desired, a junction from waveguide to Microstrip is recommended (Fig. 21).

#### Matched Load and Attenuator Pads

Matched loads and attenuator pads can be made simply by pressing a resistive card against the Microstrip conductor. For high values of attenuations, the conductor

can be interrupted and covered with a lossy material. For good stability in the values of attenuation, precision metallized films on glass can be used instead of the common resistive cards which are more subject to the influences of temperature and humidity.

### Corners and Bends

Fig. 22 shows the variation of the input VSWR produced by different cuts in a right-angle bend. As can be seen, a  $45^\circ$  cut or a smooth round corner will produce no appreciable reflection. The radiation loss for a round corner is less than 0.1 db at 5000 mc. Right-angle bends in the third dimension are also possible with small reflection and small losses.

### Impedance Matching Transformers

Tapers. A relatively frequency insensitive match between two impedances can be obtained by using a length of tapered Microstrip line, the impedance of which, at each end is equal to the impedance to be matched at that end (see Fig. 23). The curves of  $Z_0$  versus the width of the strip conductor (Fig. 10) are useful for such designs.

Stubs. Microstrip stub sections in shunt with the main line behave like shunt reactance. The reactance can be either inductive or capacitive and can have any value between zero and a maximum value. This maximum value is limited by the losses in the line, and depends on whether the end of the stub is left open or short-circuited and also upon the length of the stub. Fig. 24 shows the VSWR produced by a short-circuited stub, as a function of frequency. The stub sections can be used as variable impedance transformers to introduce a known impedance at some point in the line, or to match a line when the output is terminated in any arbitrary impedance. Double-stub and triple-stub transformers can also be designed in a similar fashion to multiple-stub coaxial tuners.

Microstrip Step Discontinuity. Experiments show that the equivalent circuits of a Microstrip step discontinuity is an ideal transformer if the losses in the lines are small. Fig. 25 shows the values of the square of the turn ratio  $n$  of the equivalent transformer as the width of one of the lines is varied. In a first approximation:  $n^2 = Z_2/Z_1$ , where  $Z_2$  and  $Z_1$  are the characteristic impedances of the two lines. Due to the non-dispersive properties of Microstrip, this type of discontinuity is rather insensitive to frequency.

Transverse Posts. Transverse posts may be used in Microstrip not only as impedance transformers for matching purposes, but also as means for providing d-c paths between the strip conductor and the ground plane. This d-c path is necessary in some applications, i.e., in crystal holders to insure a closed circuit for the rectified d-c flowing through the crystal.

As a first approximation, the susceptance of a transverse post varies with frequency like the susceptance of a pure inductance.

Due to radiation loss which can be appreciable for large post diameters, it is desirable to specify the susceptance of a post by its scattering matrix coefficients in which the reference plane is taken at the axis of the post. These coefficients can be deduced from the circle diagrams<sup>9,7</sup> (Fig. 26). An exact equivalent network (for the frequency used in the measurements) can also be deduced from the circle diagram as shown in Fig. 27.<sup>9</sup> Fig. 28 shows the variation of the equivalent normalized susceptance versus the diameter of the post and Fig. 29 shows this variation versus the location of the post across the line.

### Resonant Section in Microstrip

By placing two obstacles in Microstrip at the proper distance, a resonant section can be obtained.<sup>7</sup> Fig. 30 shows an example with transverse posts. In this case, the dielectric in the line was Fiberglas G-6 (a lossy dielectric at 5000 mc), the loaded Q was of the order of 23, and the unloaded Q of the order of 165. However, by removing the dielectric in the resonant section, and by proper shielding of this section, higher values of Q can be obtained.

### Hybrid Rings

The hybrid ring circuit (or magic T equivalent in waveguides) is an important component for microwave circuits such as balanced mixers, A.F.C., duplexers, etc. Using Microstrip, hybrid rings can be realized in a number of ways (see Fig. 31). In Fig. 31A one of the lines is three-quarter wavelength long and the characteristic impedance of the ring section is  $\sqrt{2}$  times the characteristic impedance of the side-arms. In Fig. 31B the side arms are folded inside the ring, providing a more compact configuration. In Fig. 31C the hybrid ring is made with T junctions separated by quarter wavelength sections of line. The characteristics at "X" band of a hybrid ring as depicted in Fig. 31A are shown in Fig. 32. At very high frequencies the width of the line is

no longer a small fraction of the wavelength, and as the ring diameter becomes smaller, a correction factor has to be applied to determine the mean diameter of the ring for optimum decoupling between opposite arms at a given center frequency. This correction factor has been determined experimentally.

#### Directional Couplers

Various types of directional couplers can be used in Microstrip. A wide-band directional coupler made with parallel-coupled Microstrip (Fig. 33) makes use of the characteristic that power flowing in one direction in the main transmission line induces a power flow in only one direction in the secondary transmission line. With this type of coupler, the coupling and directivity are a function of the distance between the parallel lines, the angle of coupling, the length of the coupling section, and the width of the lines. Thus, a large number of parameters can be used for any particular design.

#### Crystal Holders

Fixed-tuned Microstrip crystal holders for mixer applications have been developed for all frequency bands from 900 mc to 10,000 mc. The useful bandwidth of a crystal holder matched to a 50-ohm Microstrip line depends on the characteristics of the matching elements. For a wide-band holder, a tapered line is indicated, but for narrow-band applications, a simple shunt susceptance may be adequate.

The crystal holder generally used in Microstrip is mounted at right angles below the ground plane (Fig. 34). Matching is achieved by the proper location of a stub line across the main line. The stub line is short-circuited with a transverse post at the end of the line. This provides the necessary d-c return path for the rectified crystal current in case the strip conductor is d-c insulated from the ground plane. The r-f is by-passed by means of a built-in coaxial capacitor in the holder's mount.

The input VSWR for such a crystal holder is particularly low over a wide band of frequencies at "C" band (see Fig. Fig. 35). Good match is obtained with either 1N23C crystals or 1N23CR reversed crystals. At "S" band or "X" band, a somewhat reduced bandwidth is obtained, but the VSWR is less than 1.5 over a 10 to 15% bandwidth.

The problems of wide-band matching of crystal holders in Microstrip are considerably simplified with the use of crystals having r-f impedances close to 50 ohms. Development work now in progress

shows very promising results in that direction.

#### Special Microstrip Components

A large number of Microstrip components have been developed such as impedance bridges, phase modulators, coupled high-Q cavities, rotary switches, waveguide or coaxial Klystron mounts, matching sections for traveling-wave tubes, T junctions for duplexers, wide-band T junctions, etc. However, due to the space requirements of this paper, we will omit most of the above components, and discuss the use of gas discharge in Microstrip as a modulator or as a wide-band source of noise, and the use of Ferrite in Microstrip as an amplitude or phase modulator. Although both applications have been used in waveguides, Microstrip offers a broader frequency range of operation as well as more compact packaging.

#### Microstrip Gas Diode

A flat gas diode, approximately 1/16-inch thick and 3 inches long, is mounted between the strip conductor and the ground plane (Fig. 36). The line is terminated in wide-band coaxial transducers. The first tube tested was mounted with a hot cathode and a large glass bulb serving as a reservoir of gas (see Fig. 37). Actually, this is not necessary and a simple two-electrode, cold-cathode-diode, can be used just as well. Various gases were tested, but only the results obtained with Neon (pressure: 1 mm Hg) will be reported here.

Amplitude Modulator. By varying the d-c discharge current in the tube, a variable amount of attenuation can be obtained (Fig. 38). This effect can be used as amplitude modulation, or in switches in systems where the signal to noise ratio is not too important since a large amount of modulation noise is produced by the tube.

Wide Band Noise Source. In the standard waveguide gas discharge noise source, at least six different waveguide sizes are used to cover the frequency range from 1000 mc to 10,000 mc. With the Microstrip gas diode this frequency band can be covered with the same tube. In Fig. 39 the effective electron temperature in decibels above 290°K is plotted against frequency. This effective electron temperature gives the actual amount of white noise power which is available at the transducer at the input of the line, and includes the losses in the line and the losses in the transducer (the other end of the line is terminated in a matched load).

The noise output power as a function of the dc in the discharge is shown in Fig. 40. What makes the Microstrip noise diode attractive, besides its small size, is the relatively small amount of current necessary to reach the plateau of the curve.

#### Ferrites in Microstrip

Ferrites have been used in waveguides for amplitude modulation, phase modulation, and non-reciprocal effects. Similar effects can be produced with Ferrites in Microstrip, with the difference that here the Ferrite sample is usually very small and the magnet necessary to produce the field requires a small amount of current. The Ferrite sample is placed between the strip conductor and the ground plane. Fig. 41 shows the increase in attenuation produced in Microstrip at various microwave frequencies and various values of the magnetic field (H parallel to the strip conductor) for a Ferrite sample: Ferroxcube 4E. It can be seen that, as the microwave frequency increases, the peaks of the attenuation curves occur at greater magnetostatic fields, which is in qualitative agreement with the formula for ferromagnetic resonance.<sup>12</sup>

$$\omega_0 = \gamma(BH)^{\frac{1}{2}}$$

Phase shift variations can also be produced as shown in Fig. 42. Non-reciprocal effects have been observed when placing the Ferrite sample on the edges of the strip conductor.

#### Microstrip Wiring Applied<sup>6,11</sup> to Microwave Receivers

As examples of practical realizations using various Microstrip components previously described, the radio-frequency heads of various broad-band, super-heterodyne microwave receivers will be shown and compared with the equivalent conventional waveguide receivers.

Fig. 43 shows the r-f head of a single-ended mixer operating at a center frequency of 2000 mc. The local oscillator injection is made through a Microstrip directional coupler. This leads to a very simple layout on the chassis. However, the possibilities of Microstrip are more fully appreciated when the r-f circuitry is more complicated. With Microstrip, bulky waveguide flanges or coaxial type connectors necessary for the assembly of the more familiar waveguide and coaxial components can be eliminated, and the whole radio-frequency head can be manufactured as a single unit. This is shown in Fig. 44, which is a photograph of

two complete receivers on the same scale, one utilizing conventional waveguide plumbing and the other the Microstrip equivalent. This receiver uses a balanced mixer with a hybrid ring and has an automatic frequency control for the local oscillator. This AFC is of the type described by Pound,<sup>13</sup> and uses two more hybrid rings. The schematic diagram (Fig. 45) is almost a reproduction of the Microstrip print and the various Microstrip components are easily recognizable. The performances of both receivers are almost identical. The over-all weight of the conventional receiver is approximately 32 pounds; the weight of the Microstrip equivalent is under 5 pounds.

Fig. 46 shows the front view of a similar receiver operating at the center frequency of 6000 mc. A front cover can be placed permanently and can serve both as a dust cover and as an over-all shield. All the adjustments and servicing can be made from the back of the receiver (see Fig. 47). On the ground plane are mounted the Klystron local oscillator, the i-f preamplifier, the tunable reference cavity and the various crystal mixers and crystal detectors. Since the dielectric support for the Microstrip is attached to a solid conducting ground sheet, it is possible to utilize the ground sheet as a chassis for the low-frequency circuitry; i.e., intermediate frequency, video-frequency, and automatic-frequency control amplifiers. This was already shown in Fig. 3.

The i-f impedance, the conversion loss and the mixer noise temperature are a function of the image-frequency termination. If a preselecting circuit (filter, T-R box) is used in the signal line, considerable variations in the frequency response and noise figure of the receiver can be observed over a wide band of frequencies. By making the lengths of the lines from the junction to the crystals to differ by a quarter wavelength, the balanced mixer can be so arranged that the image frequency wave is transmitted into the local oscillator arm of the hybrid ring (see Fig. 48). A matched attenuator pad in this arm allows the image frequency power to be absorbed without reflection and both crystals behave as they would in a mixer without preselecting circuit.

Wide-band r-f heads with balanced mixers have been made for center frequencies ranging from 1000 to 10,000 mc. The sensitivity of these receivers at "S" band, "C" band, and "X" band is shown in Fig. 49. The single side-band noise figure<sup>14</sup> is plotted against frequency and it can be seen that these receivers compare very favorably with equivalent receivers made with conventional waveguides.

Furthermore, with Microstrip, the design of the receivers can be standardized so as to give almost the same physical dimensions to receivers from "S" band to "X" band. On the other hand, the printing techniques for Microstrip allows accuracy of reproduction compatible with low-cost production.

#### Microstrip Kit

To introduce Microstrip and facilitate experimentation, a Microstrip Kit has been developed (Fig. 50).

The Microstrip Kit utilizes various Microstrip components as separate units. The connection between such components is made through a special clip and the whole assembly can be mounted on a simple frame (Figs. 51 and 52).

Although the final design of a Microstrip circuit will not use clip connections, the Microstrip Kit assembly can provide very quickly a good approximation on the performance of many microwave printed circuits without involving the all-printed technique.

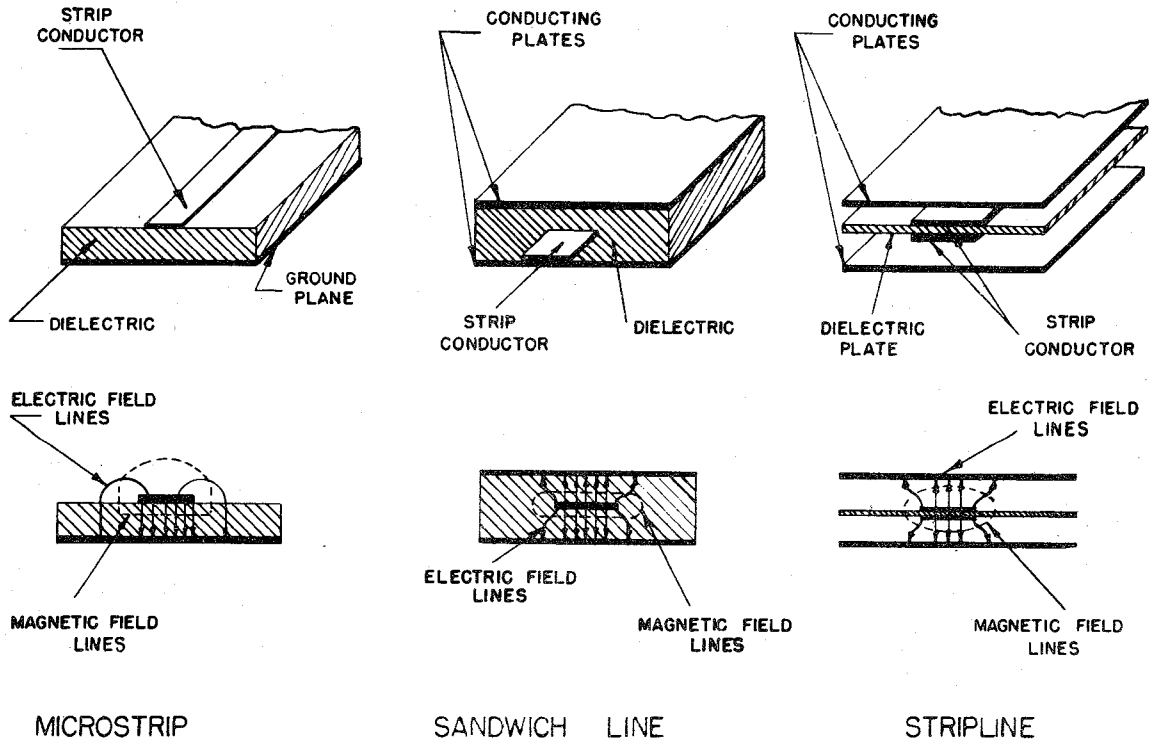
#### References

1. R. M. Barrett, "Etched Sheets Serve as Microwave Components," Electronics, vol. 25, p. 114-118; June 1952.
2. D. D. Grieg and H. F. Engelmann, "Microstrip - A New Transmission Technique for the Kilomegacycle Range," Proc. I.R.E., vol. 40, p. 1644-1650; December 1952.
3. F. Assadourian and E. Rimai, "Simplified Theory of Microstrip Transmission Systems," Proc. I.R.E., vol. 40, p. 1651-1657; December 1952.
4. J. A. Kostriza, "Microstrip Components," Proc. I.R.E., vol. 40, p. 1658-1663; December 1952.
5. M. Arditì and J. Elefant, "Characteristics of Microwave Printed Lines (Microstrip) with Application to the Design of Band-Pass Microwave Filters," IRE - ISRU Meeting, April 21-24, 1952.  
M. Arditì, "Experimental Determination of the Properties of Microstrip Components," Convention Record of the IRE, p. 27-37; March 23, 1953; reprinted in Electrical Communication, Vol. 30, p. 283-293; December 1953.
6. E. Fubini, W. Fromm, and H. Keen, "New Technique for High-Q Strip Microwave Components," Convention Record of the IRE, p. 91-97; March 22, 1954.  
"Microwave Applications of High-Q Strip Components," Convention Record of the IRE, p. 98-103; March 22, 1954.
7. K. S. Packar, "Machine Methods Make Strip Transmission Line," Electronics, p. 149-150; September 1954.
8. S. B. Cohn, "Characteristic-Impedance of the Shielded-Strip Transmission Line," Trans. of the IRE - PGMTT, Vol. MIT-2, No.2, p. 52-55; July 1954.
9. G. Deschamps, "Application of Non-Euclidian Geometry to the Analysis of Waveguide Junctions," IRE - ISRU Meeting, April 23, 1952. Published in part under the title: "Determination of the Reflection Coefficient and Insertion Losses of a Waveguide Junction," Jour. of App. Phys., vol. 24, p. 1046-1050; August 1953.  
"Geometric Viewpoints in the Representation of Waveguides and Waveguide Junctions," Proc. of the Symposium on Modern Network Synthesis, p. 277-295; September 30, 1952.  
"New Chart for the Solution of Transmission Line and Polarization Problems," Electrical Communication, vol. 30, p. 247-254; September 1953; also Trans. of the IRE - PGMTT, Vol. 1, p. 5-13; March 1953.  
"Accurate Comparison of High Standing Wave Ratio and Its Application to the Determination of Attenuation Constant of a Waveguide," presented at the Ultra-High Frequency Measurements Conference, Washington, D.C., January 16, 1953 - Unpublished.  
"A Hyperbolic Protractor for Microwave Impedance Measurements and Other Purposes," Federal Telecommunication Laboratories, Nutley, New Jersey.  
"Theoretical Aspects of Microstrip Waveguides," Trans. of the IRE - PGMTT-2, No. 1, p. 100; April 1954.
10. M. Schetzen, Quarterly Progress Reports, Research Labs Electronics, M.I.T., April 15, 1953 - April 15, 1954.
11. H. F. Engelmann, "Microstrip Wiring Applied to Microwave Receivers," Symposium on Microwave Circuitry, IRE - PGMTT, New York, November 1952.
12. G. Kittel, "On the Theory of Ferromagnetic Resonance Absorption," Physical Review, Vol. 73, No. 2; January 1948.



13. R. V. Pound, "Frequency Stabilization of Microwave Oscillators," Proc. I.R.E., vol. 35, No. 12, p. 1405; December 1947.

14. Standards on Electron Devices: "Methods of Measuring Noise," Proc. I.R.E., p. 896; July 1953.



MICROWAVE PRINTED CIRCUITS 1952

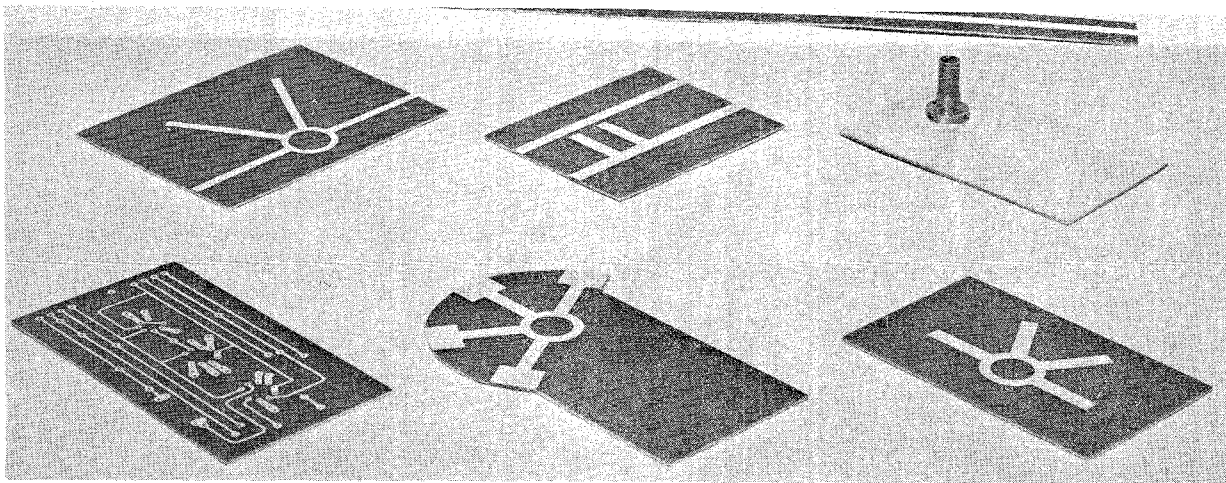


Fig. 2 - Microstrip and low frequency printed circuits.



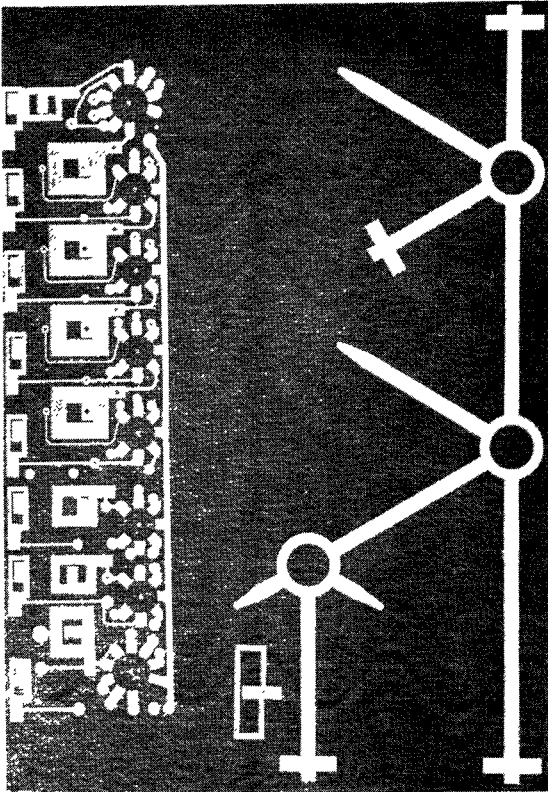


Fig. 3 - Microstrip and I-F printed circuit.

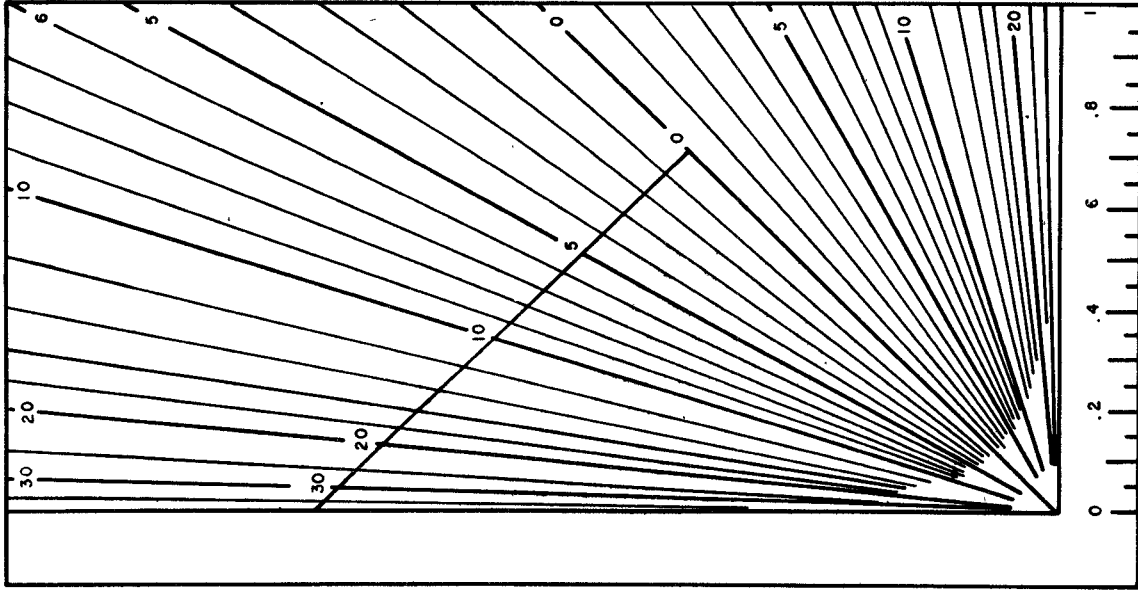


Fig. 6 - Deschamps' hyperbolic protractor.

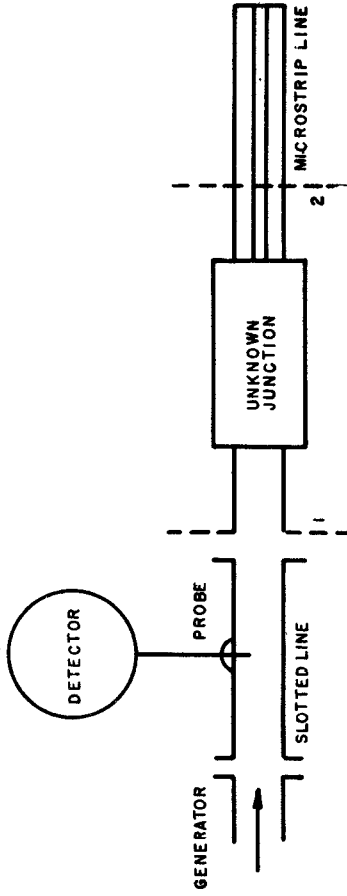


Fig. 4 - Experimental set-up.

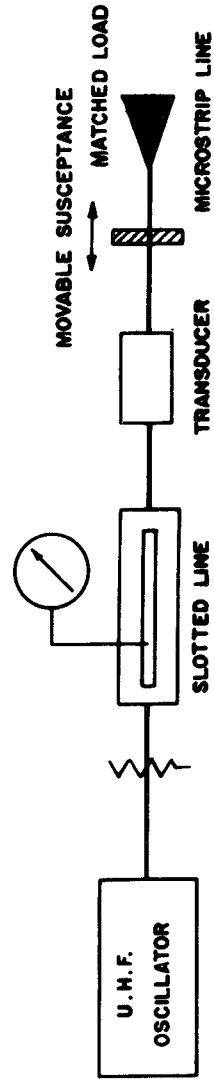


Fig. 5 - Schematic of experimental set-up.

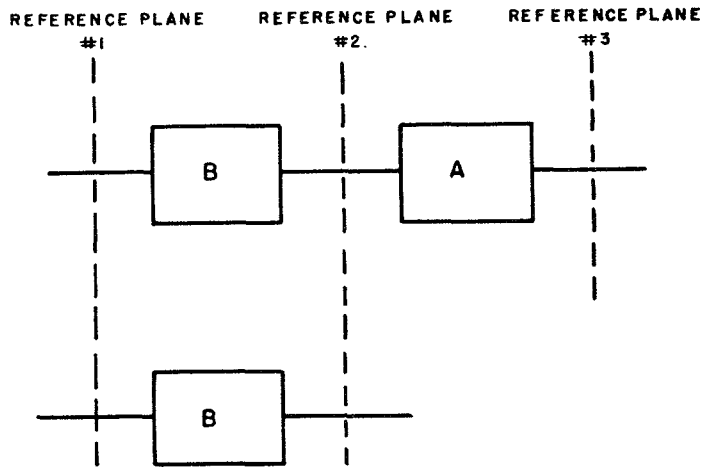


Fig. 7 - Measurement of junction A through a junction B.

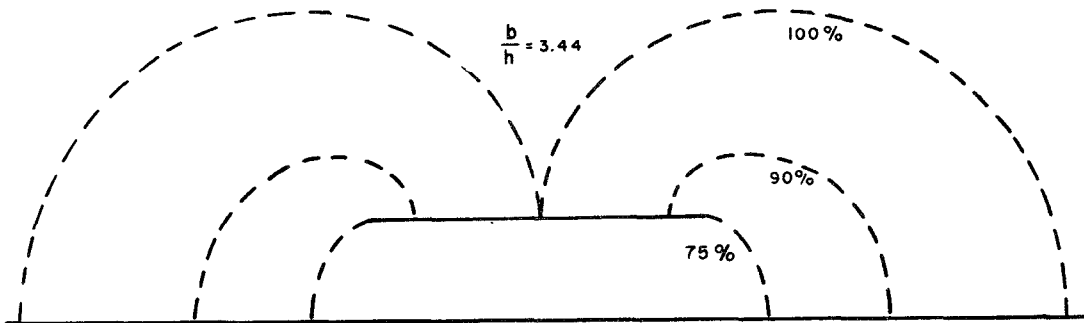


Fig. 8 - Distribution of power flow for wide strip of zero thickness above infinite ground plane.

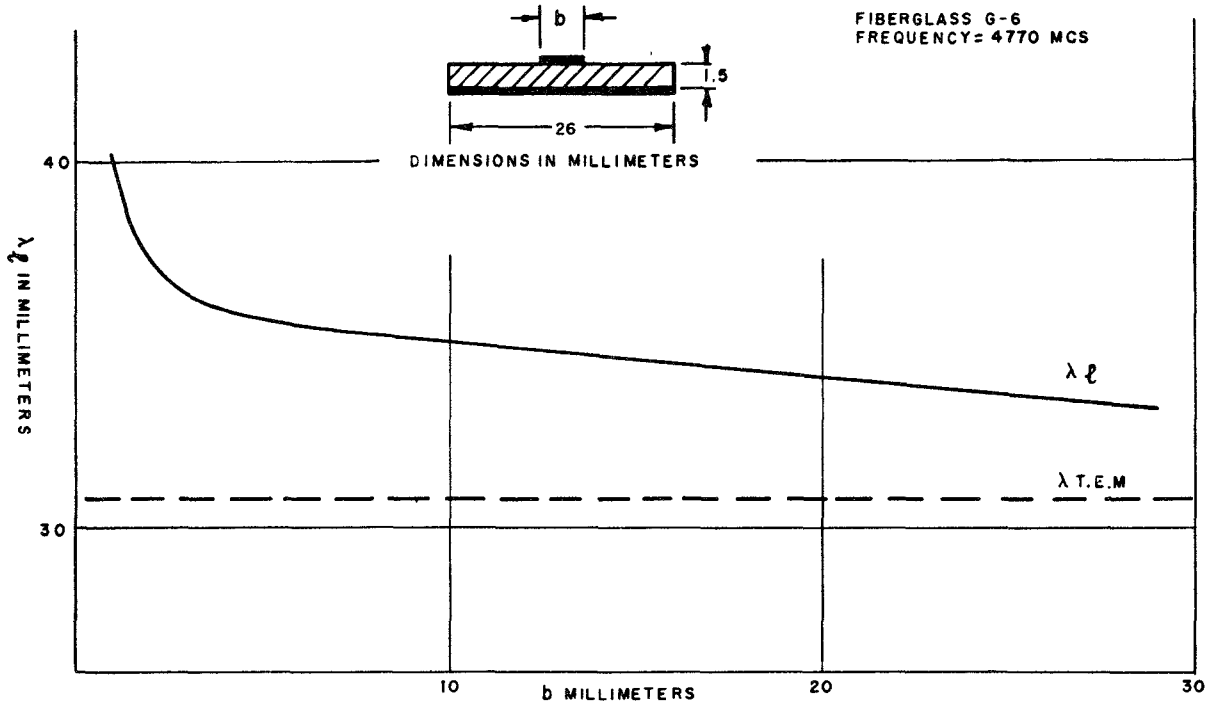


Fig. 9 - Microstrip wavelength versus width of strip conductor.

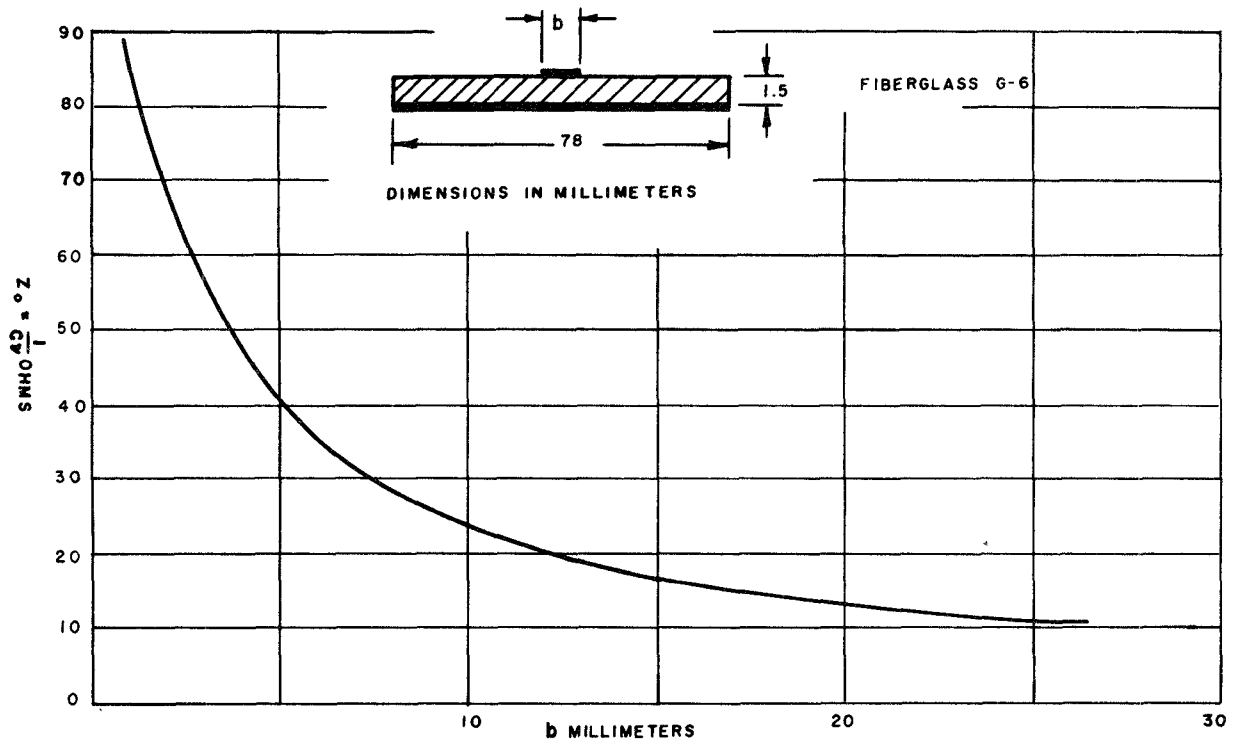


Fig. 10 - Characteristic impedance for microstrip with fiberglass base.

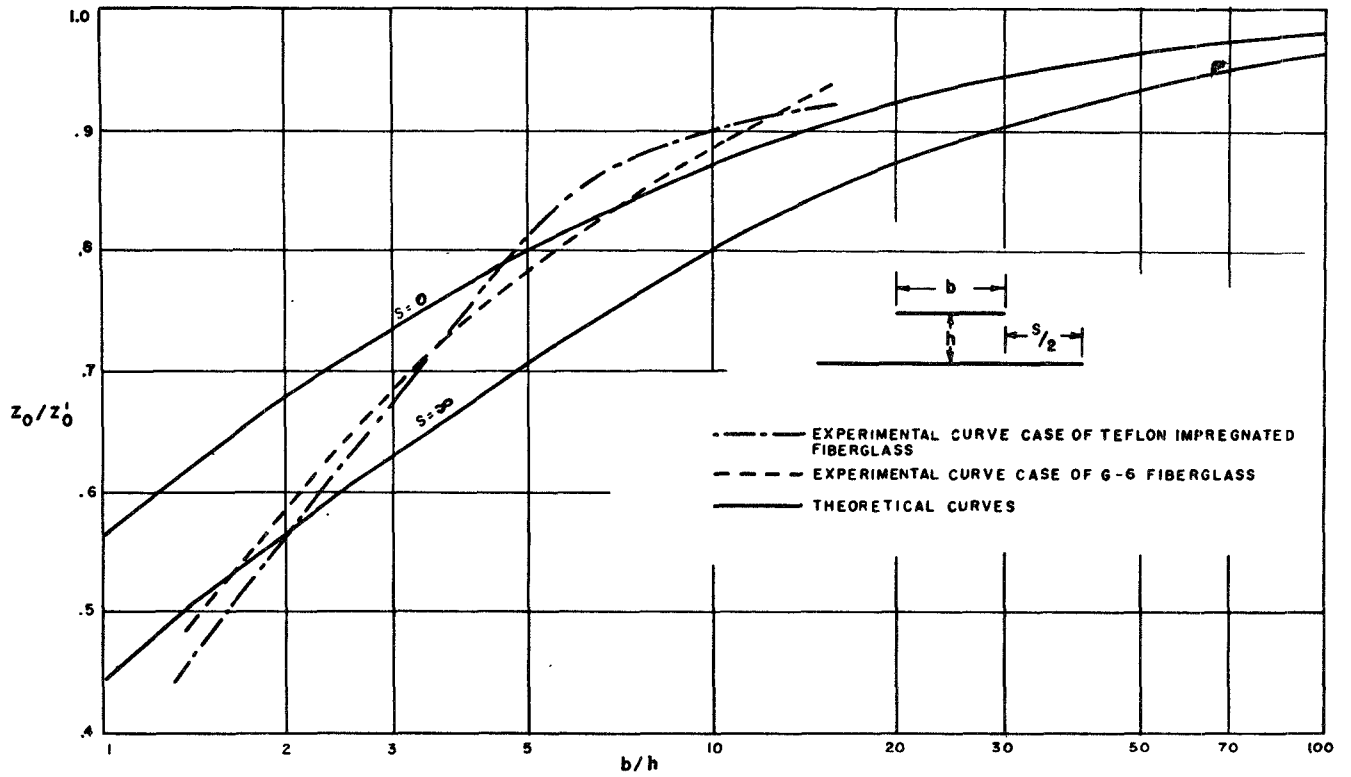


Fig. 11 - Characteristic impedance for wide strip of zero thickness above finite ground plane compared to experimental results.

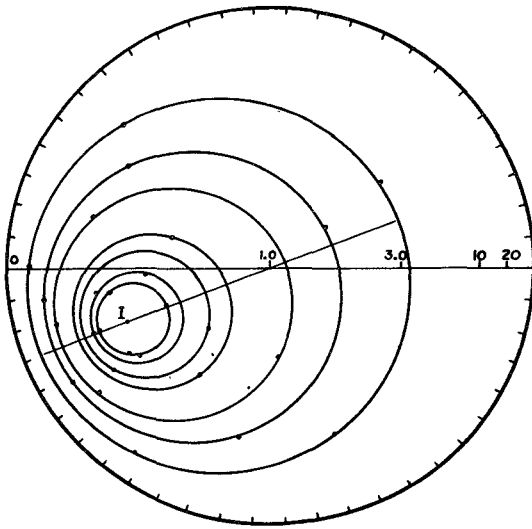


Fig. 12 - Circle diagrams for attenuation measurements.

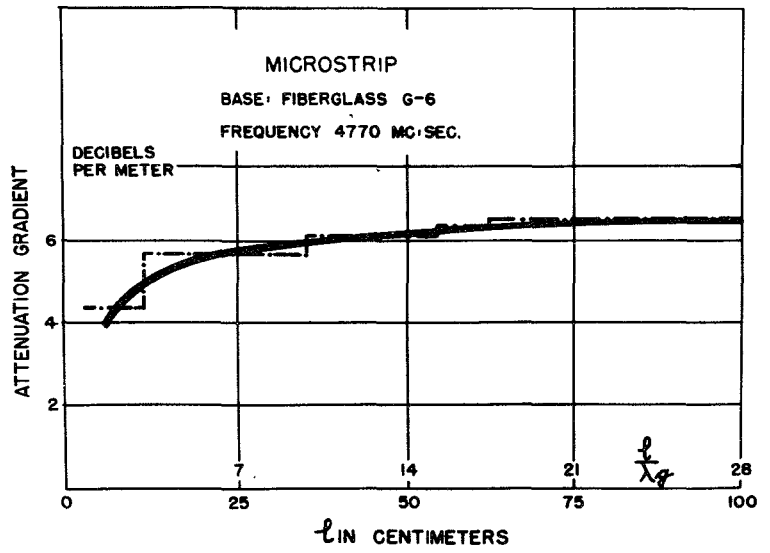


Fig. 13 - Attenuation along microstrip line.

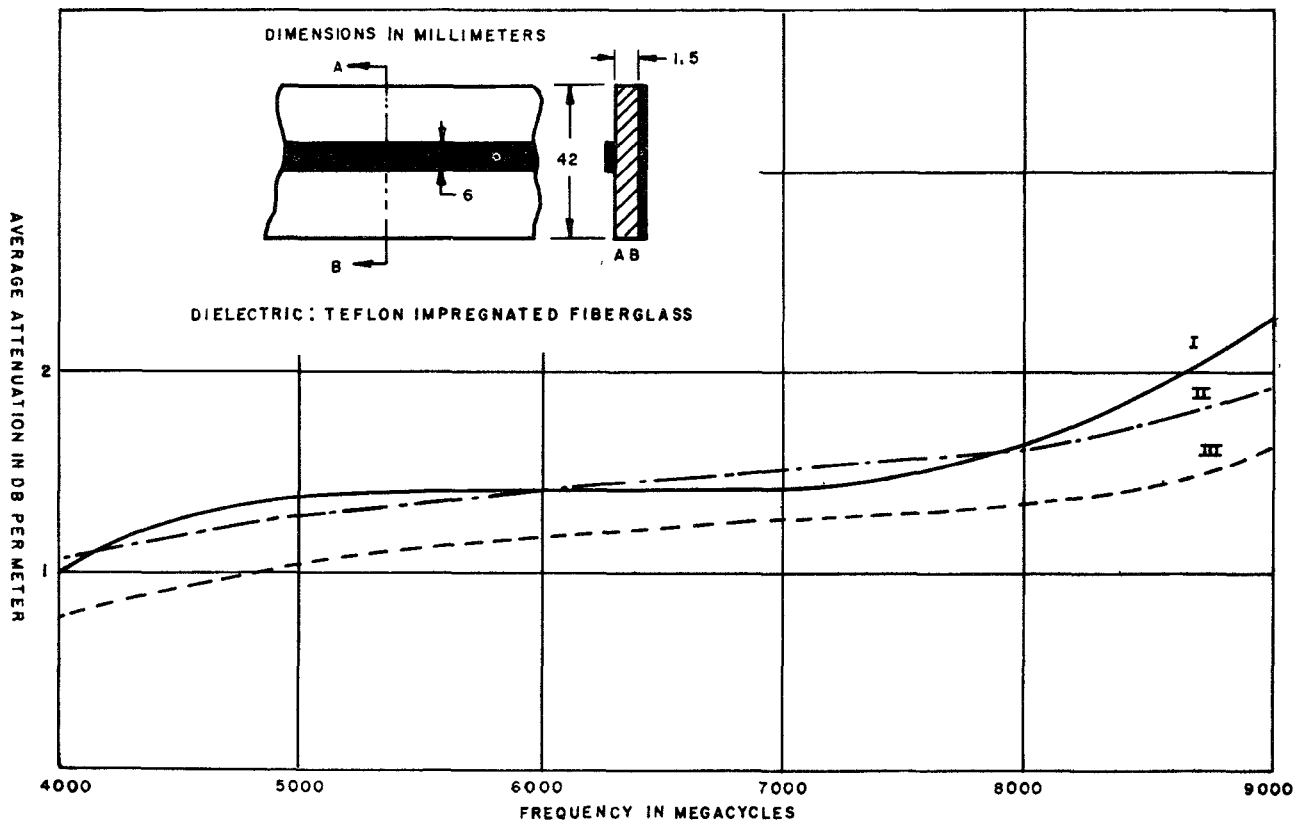


Fig. 14 - Average attenuation in microstrip versus frequency.

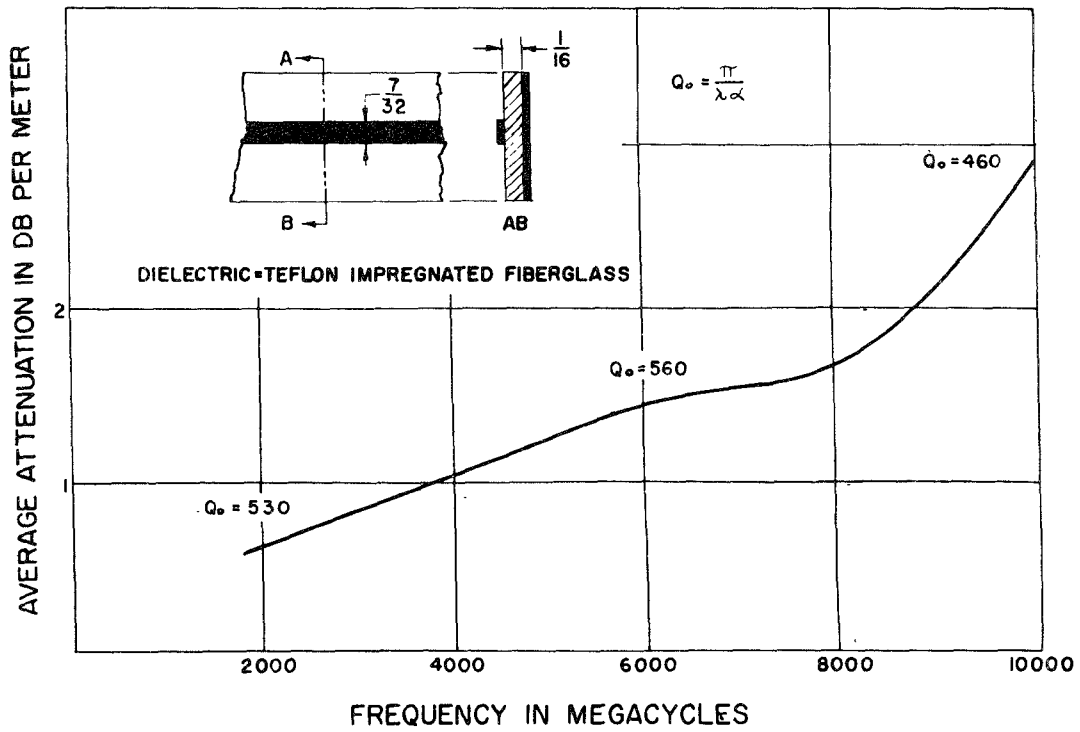


Fig. 15 - Microstrip attenuation.

FREQUENCY IN MEGACYCLES	RECTANGULAR WAVEGUIDE		COAXIAL LINE		MICROSTRIP LINE TEFLON IMPREGNATED FIBERGLASS 1/8 INCH THICK
	AIR	POLYSTYRENE	3/8 INCH AIR	RGB/U	
5000	0.021	0.18	0.070	0.25	0.33
9000	0.074	0.46	0.095	0.40	0.60

Fig. 16 - Attenuation in decibels per foot.

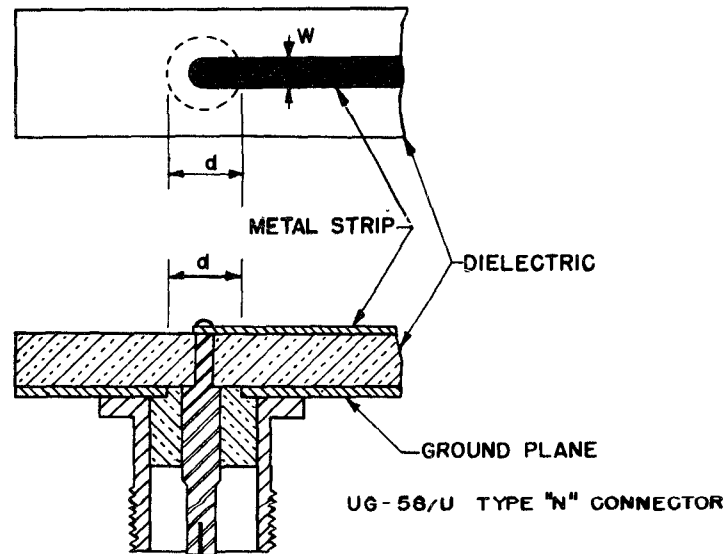


Fig. 17 - Microstrip to coaxial transducer.

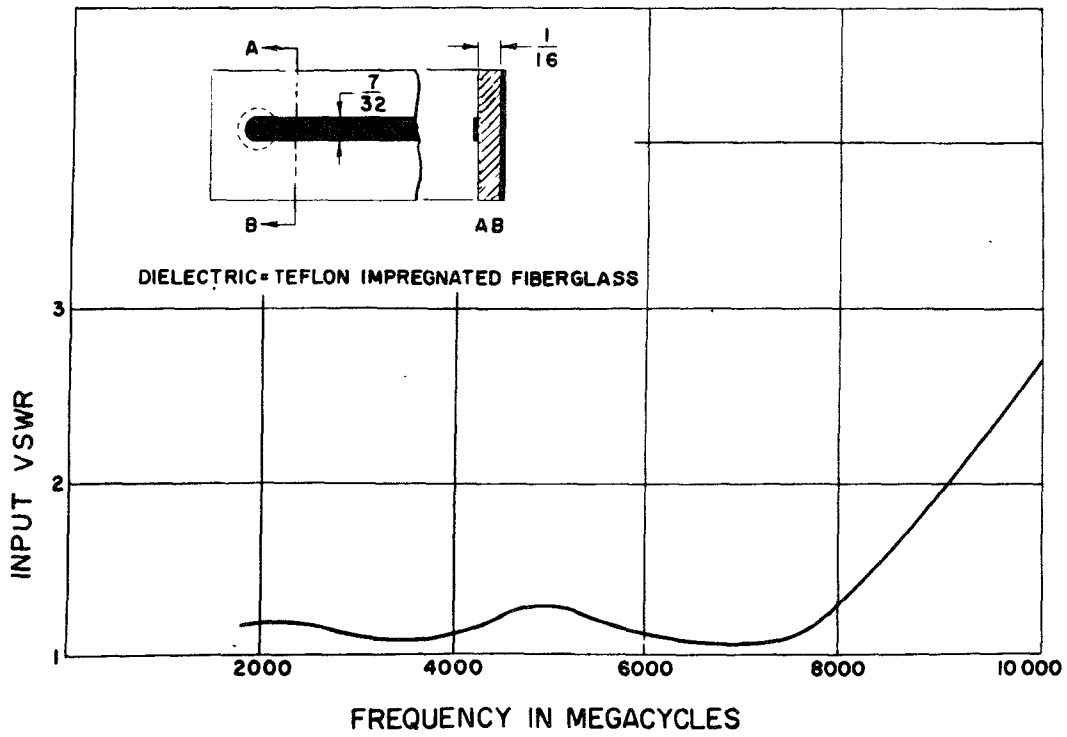


Fig. 18 - Input VSWR versus frequency for coaxial to microstrip transducer.

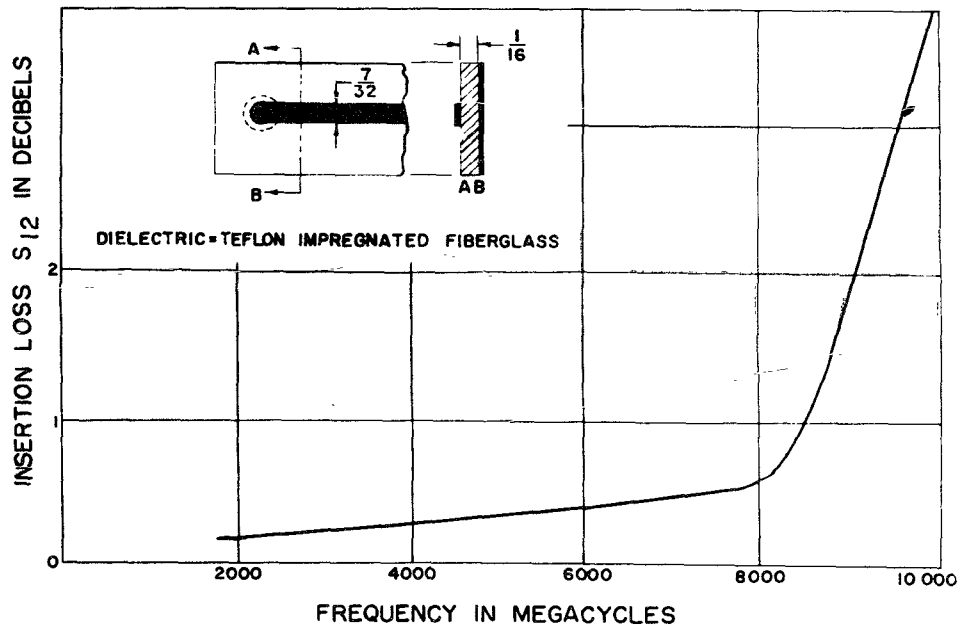


Fig. 19 - Insertion loss for coaxial to microstrip transducer.

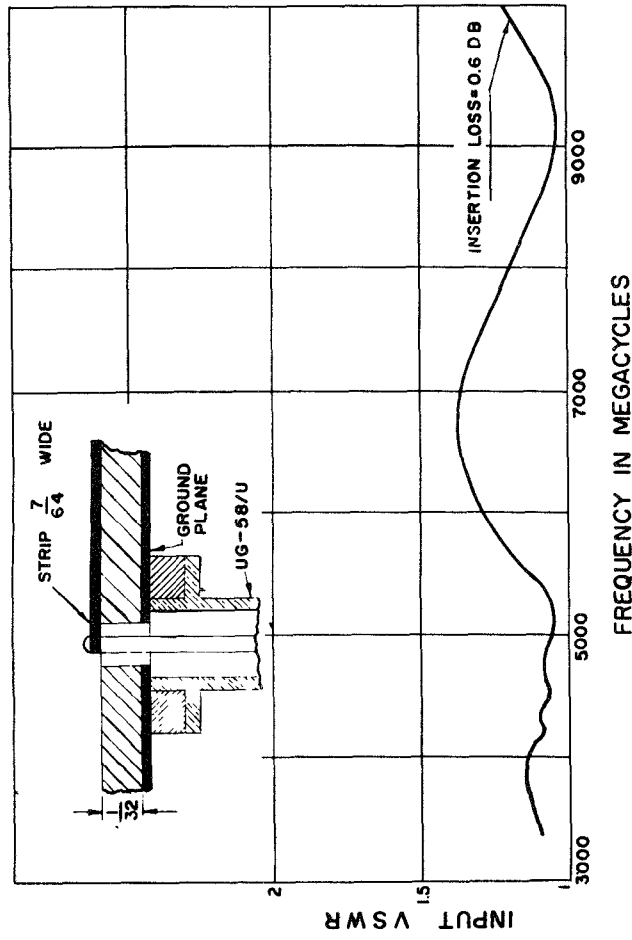


Fig. 20 - Wide-band coaxial to microstrip transducer.

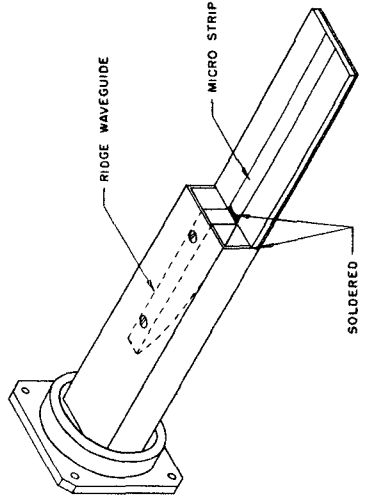


Fig. 21 - Waveguide to microstrip transducer.

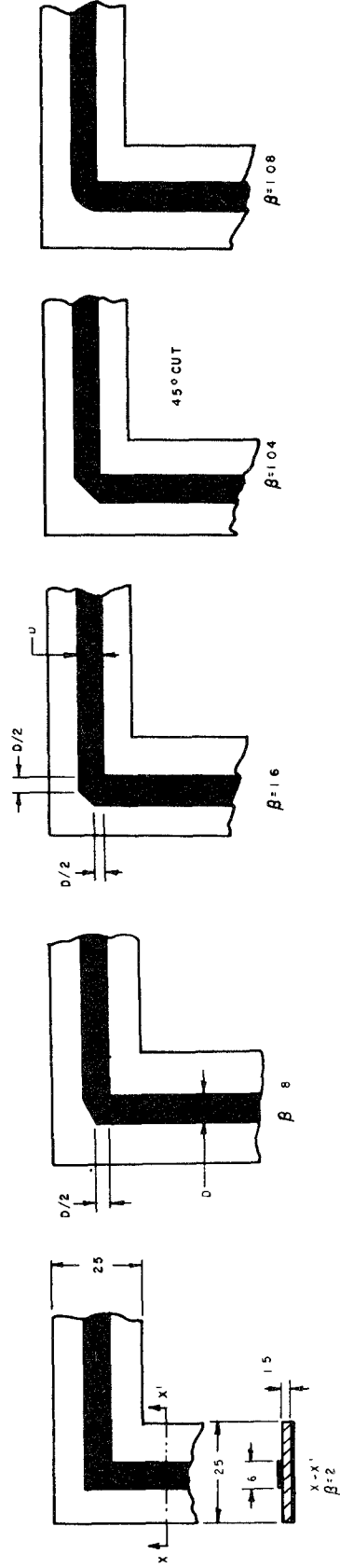


Fig. 22 - Right angle bends in microstrip.

DIMENSIONS IN MILLIMETERS  
 FREQUENCY = 4700 MC  
 DIELECTRIC = FIBERGLASS G-6  
 $\beta$  = INPUT VSWR



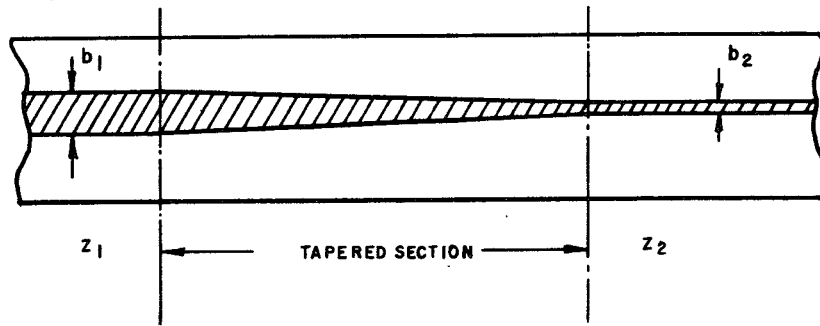


Fig. 23 - Microstrip tapered line.

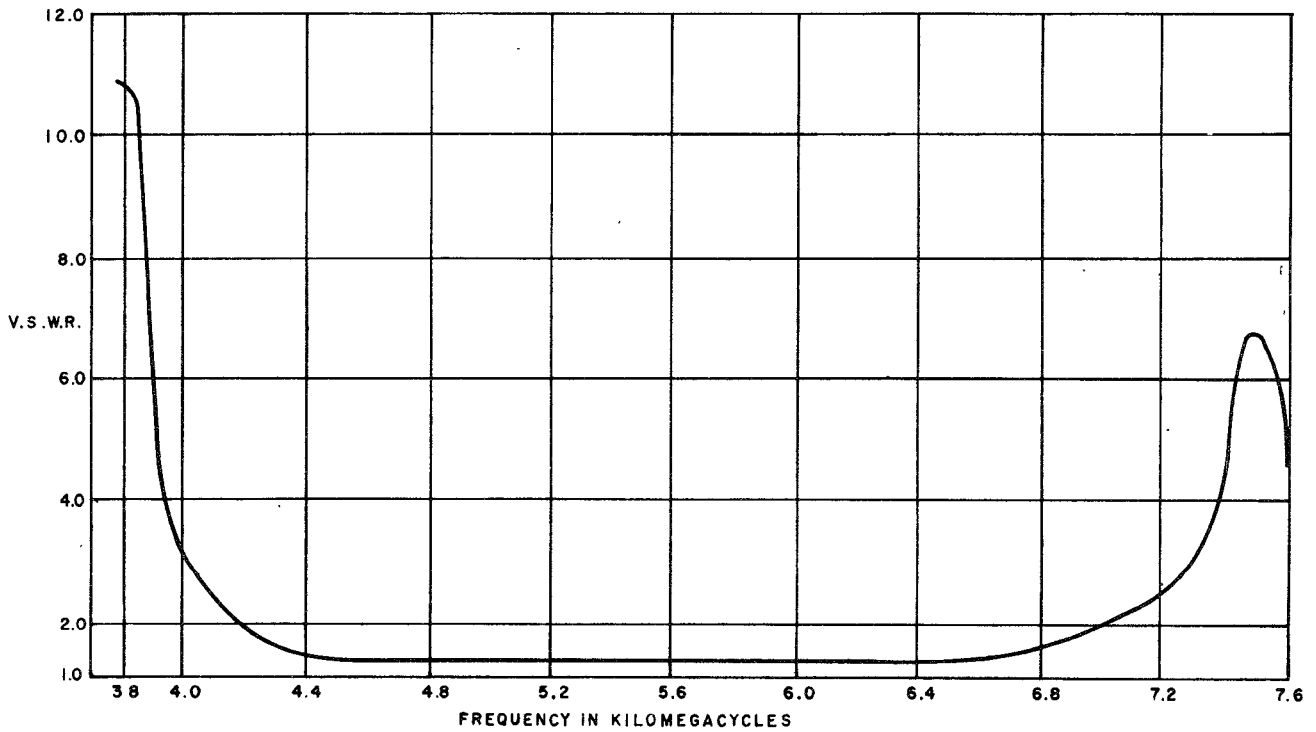
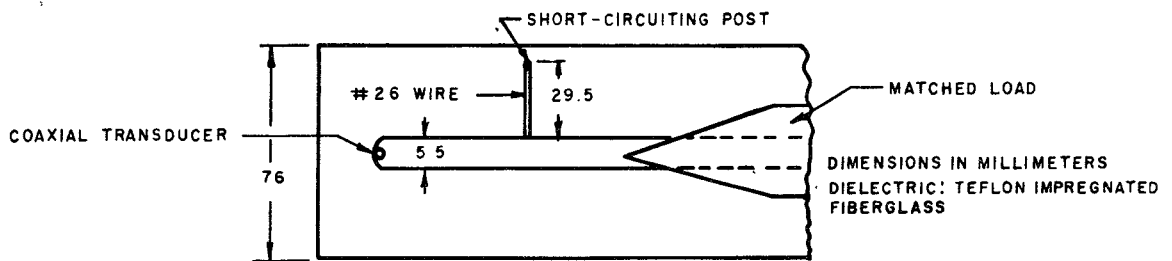


Fig. 24 - VSWR characteristic for short-circuited stub across microstrip.

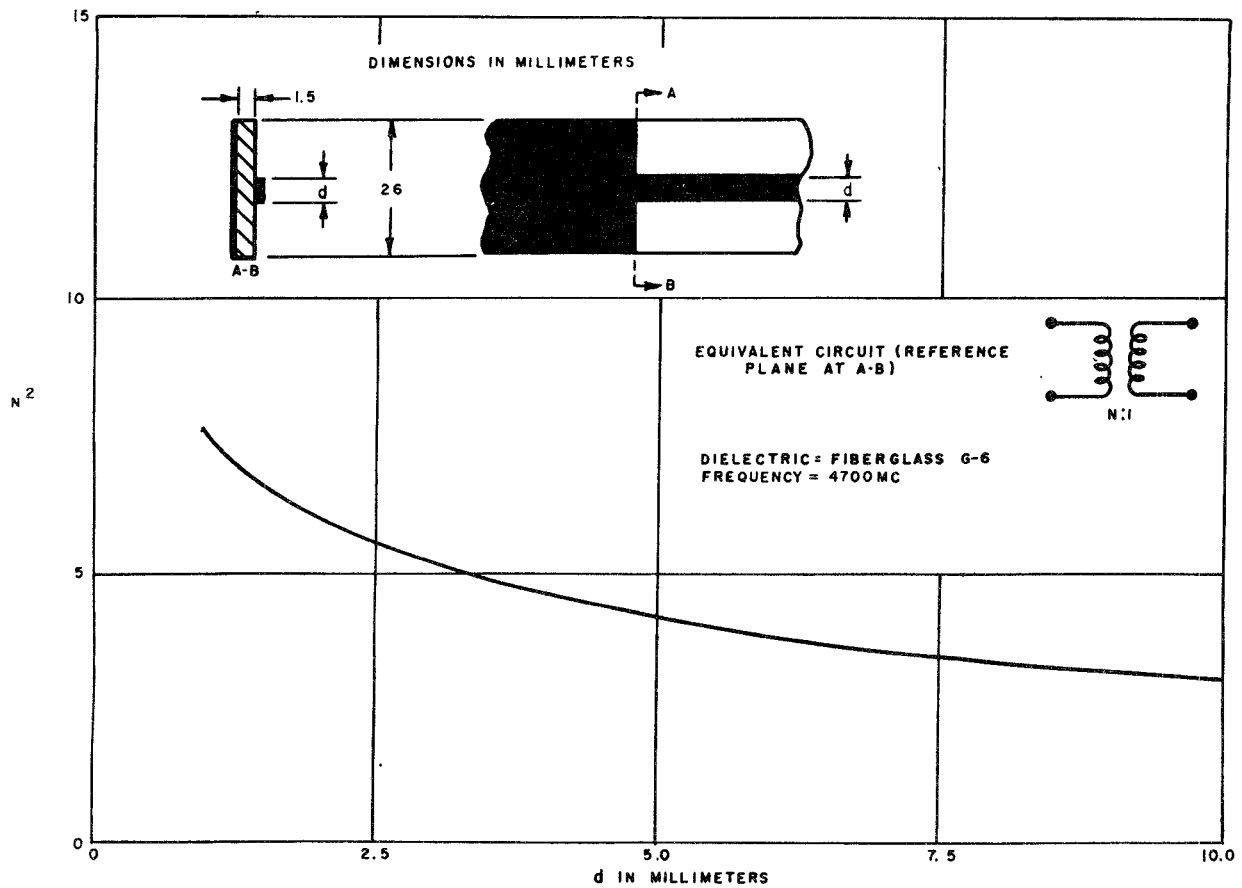


Fig. 25 - Microstrip step discontinuity.

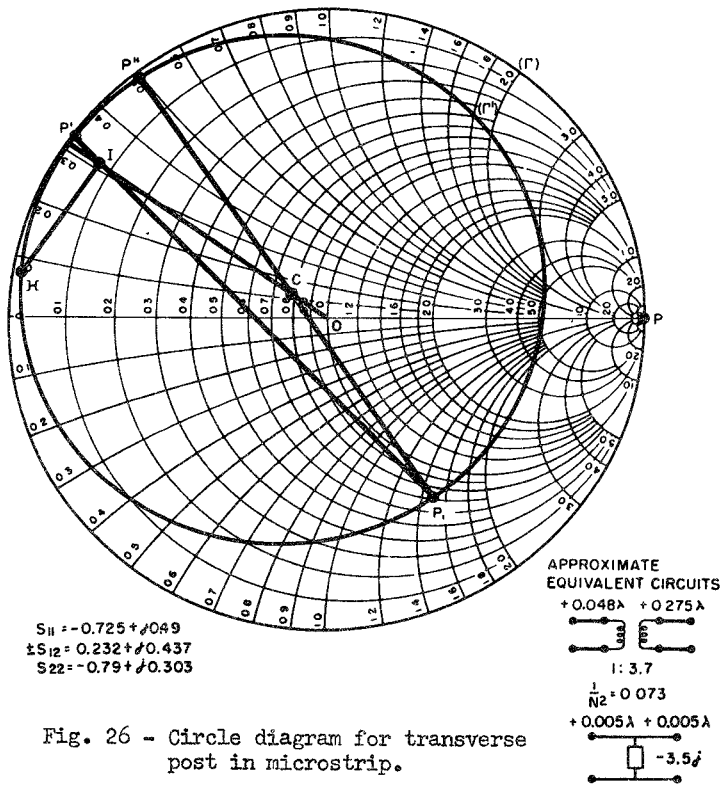
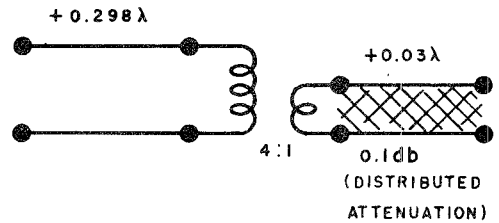


Fig. 26 - Circle diagram for transverse post in microstrip.

(a) EXACT EQUIVALENT CIRCUIT INCLUDING LOSSES



(b) APPROXIMATE EQUIVALENT CIRCUIT NEGLECTING THE LOSSES

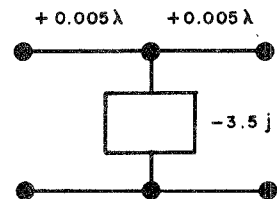


Fig. 27 - Exact and approximate equivalent circuits for post transverse to microstrip line.

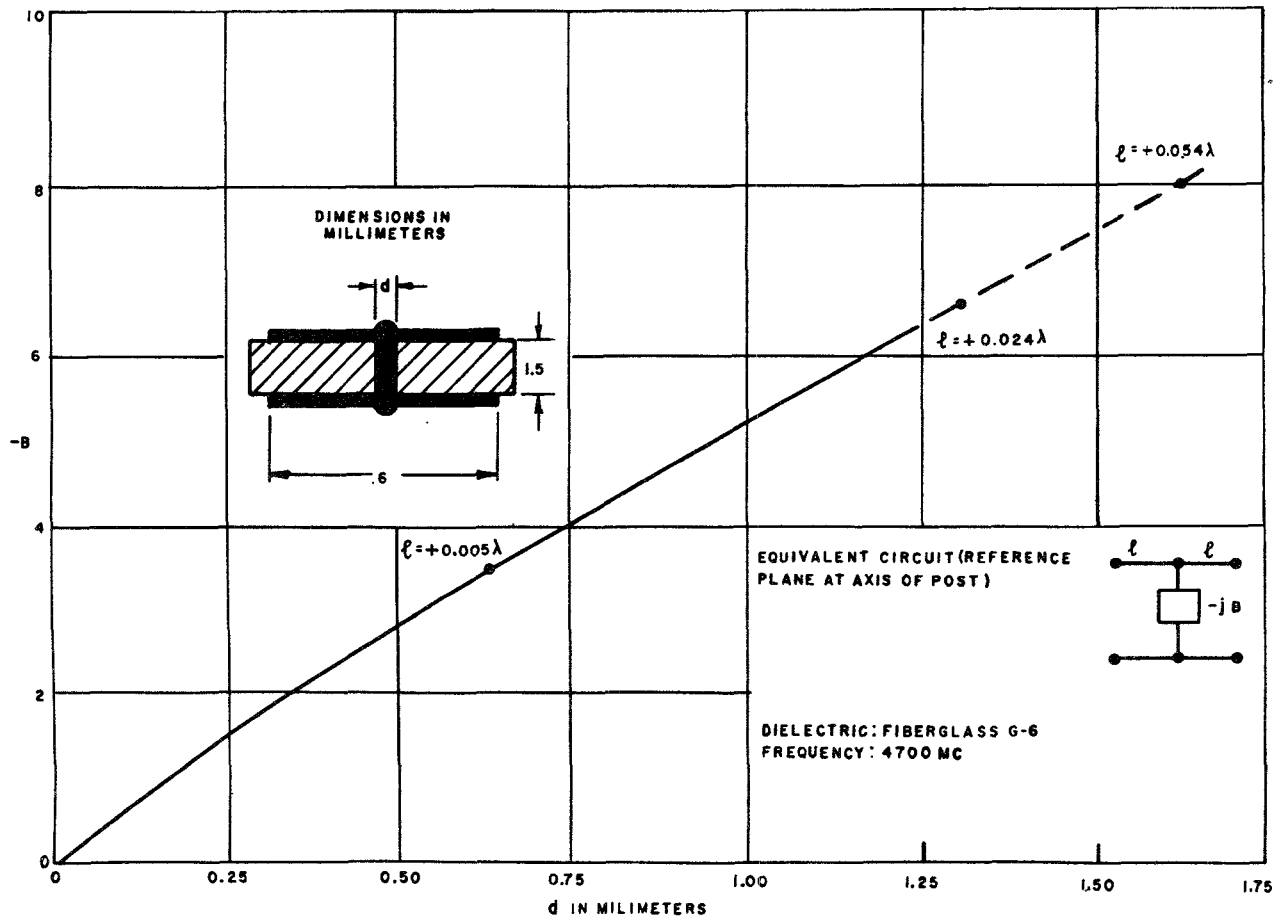


Fig. 28 - Variation of shunt susceptance with diameter of a post.

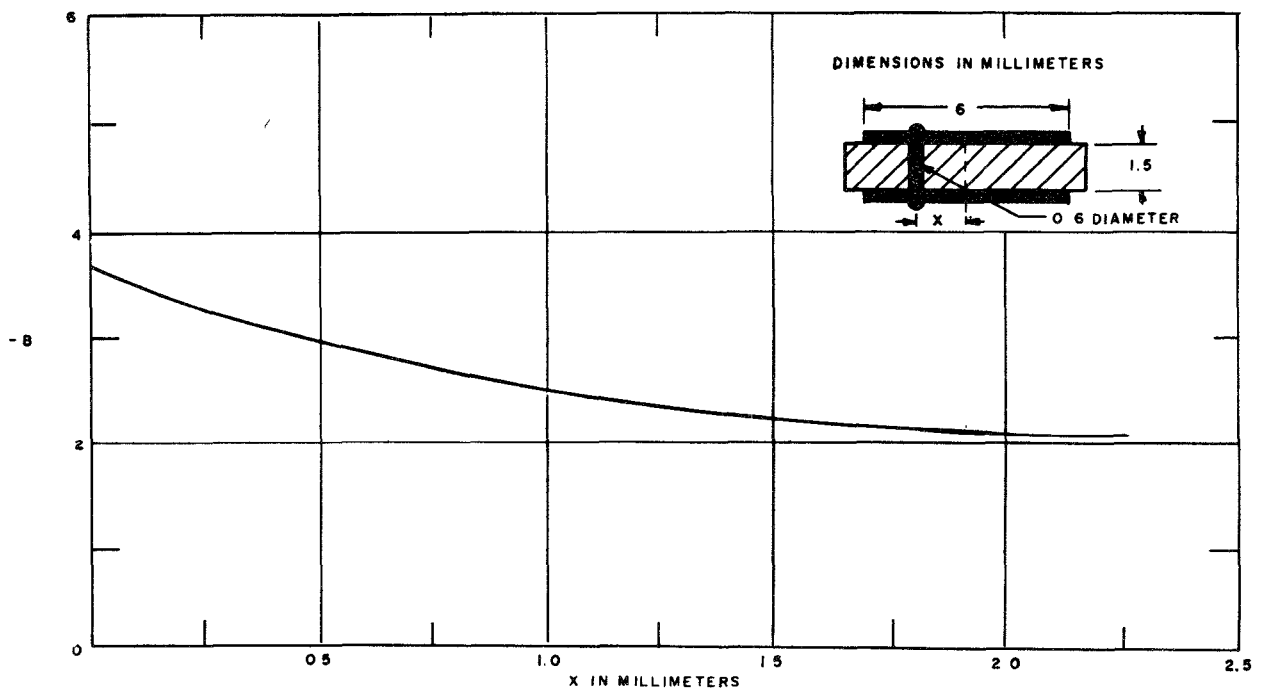


Fig. 29 - Variation of shunt susceptance with location of a post.

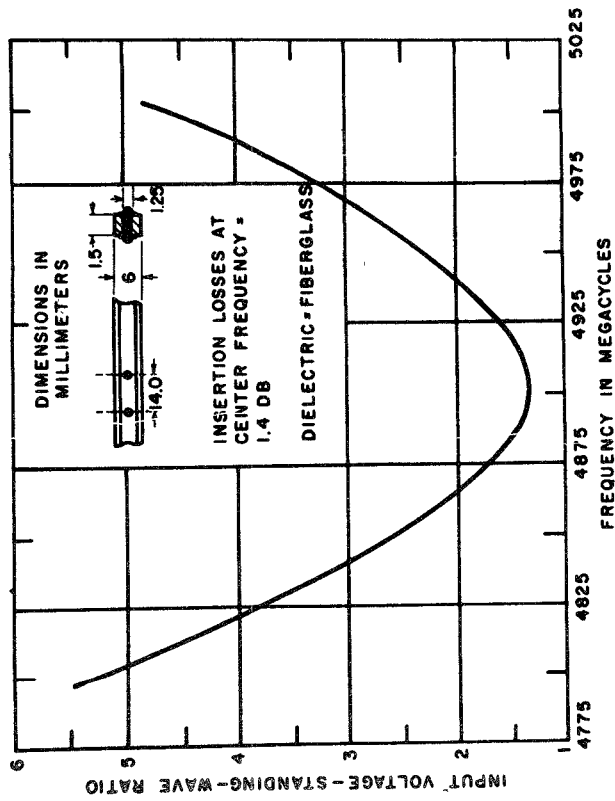


Fig. 30 - Microstrip resonant section with transverse posts.

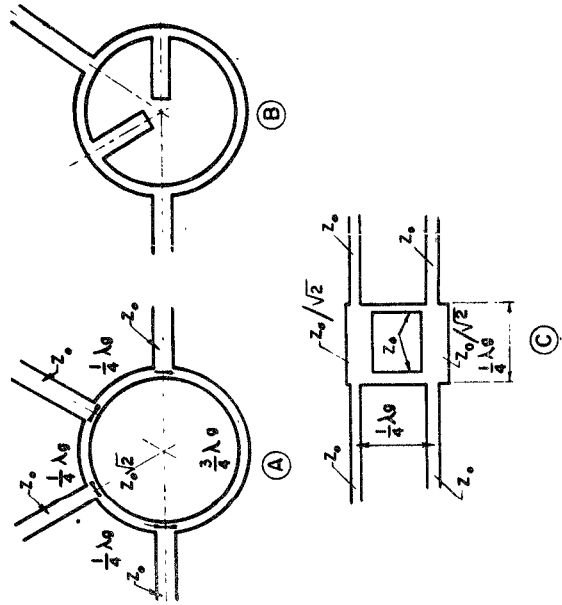


Fig. 31 - Microstrip hybrid ring.

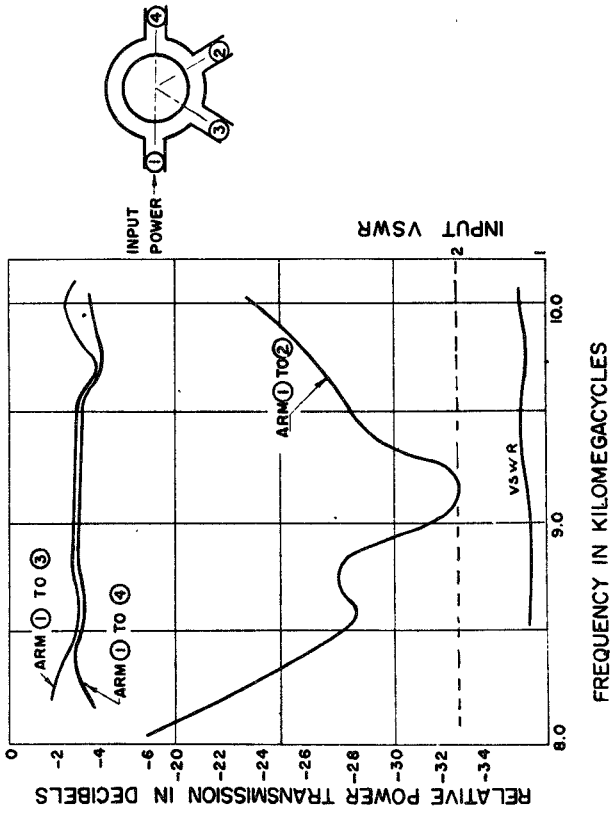


Fig. 32 - Microstrip hybrid ring for "X" band.

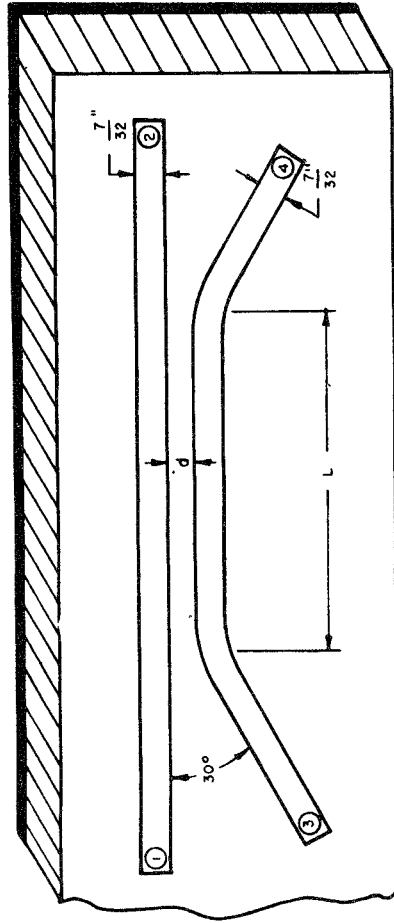


Fig. 33 - Microstrip directional coupler.

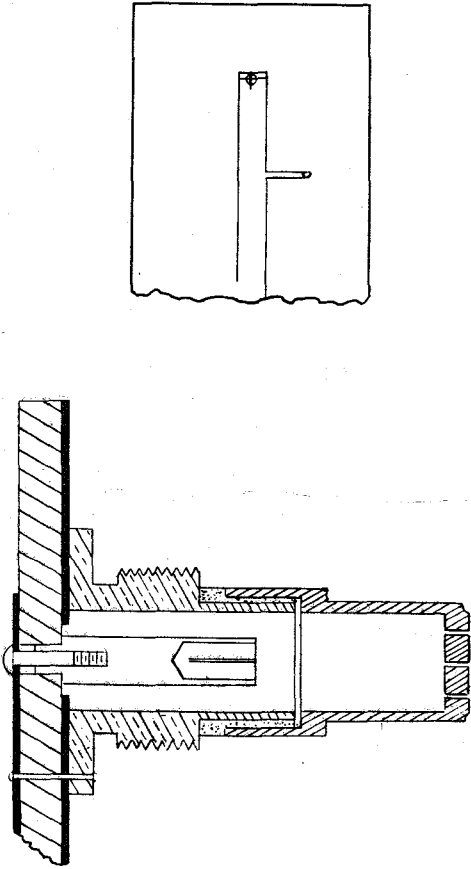


Fig. 34 - Microstrip crystal holder.

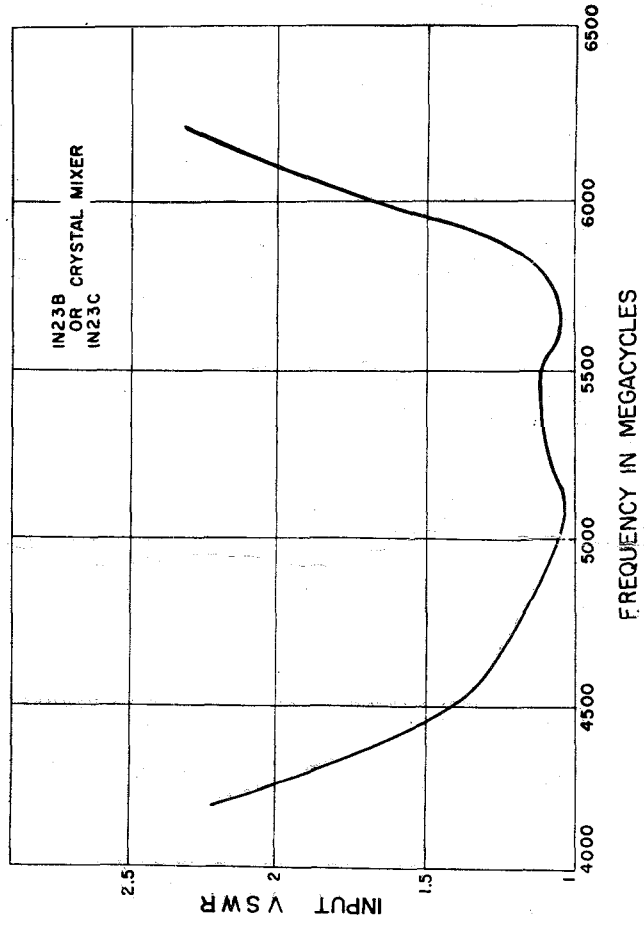


Fig. 35 - Microstrip crystal mixer at "C" band.

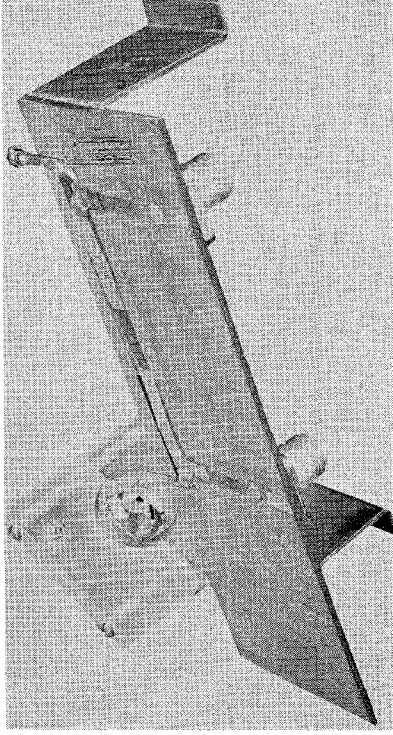


Fig. 36 - Microstrip gas diode.



Fig. 37 - Gas diode for microstrip.

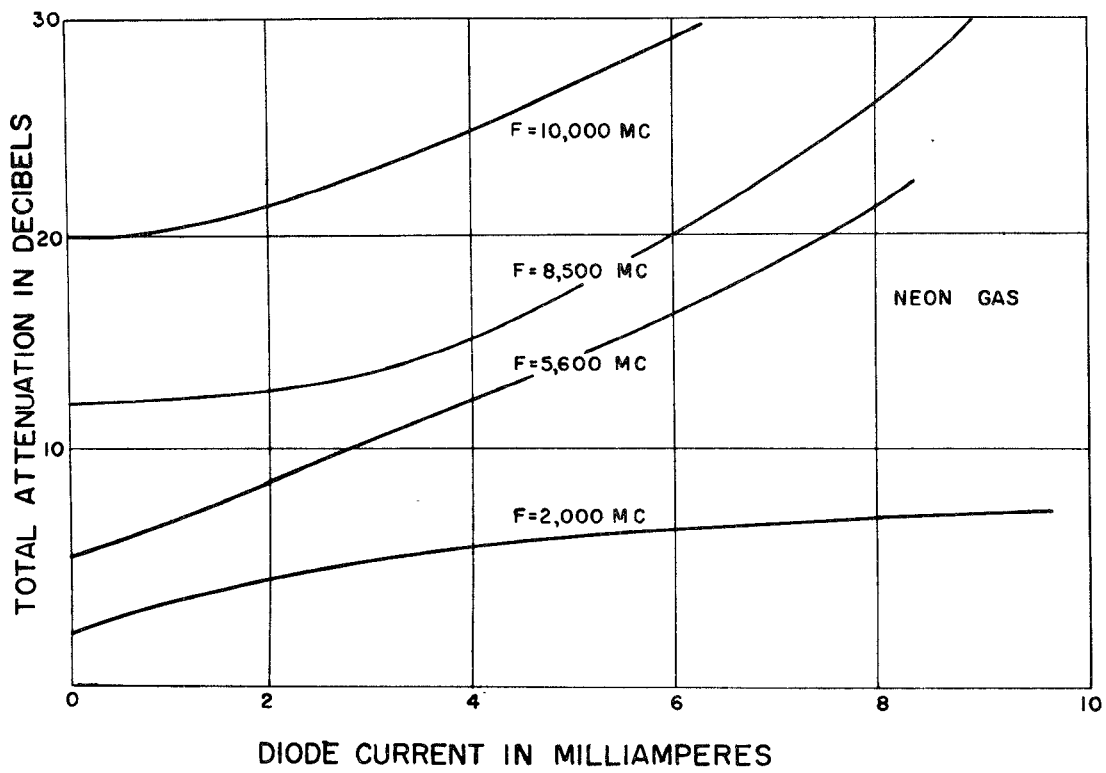


Fig. 38 - Microstrip gas diode as R-F variable attenuator.

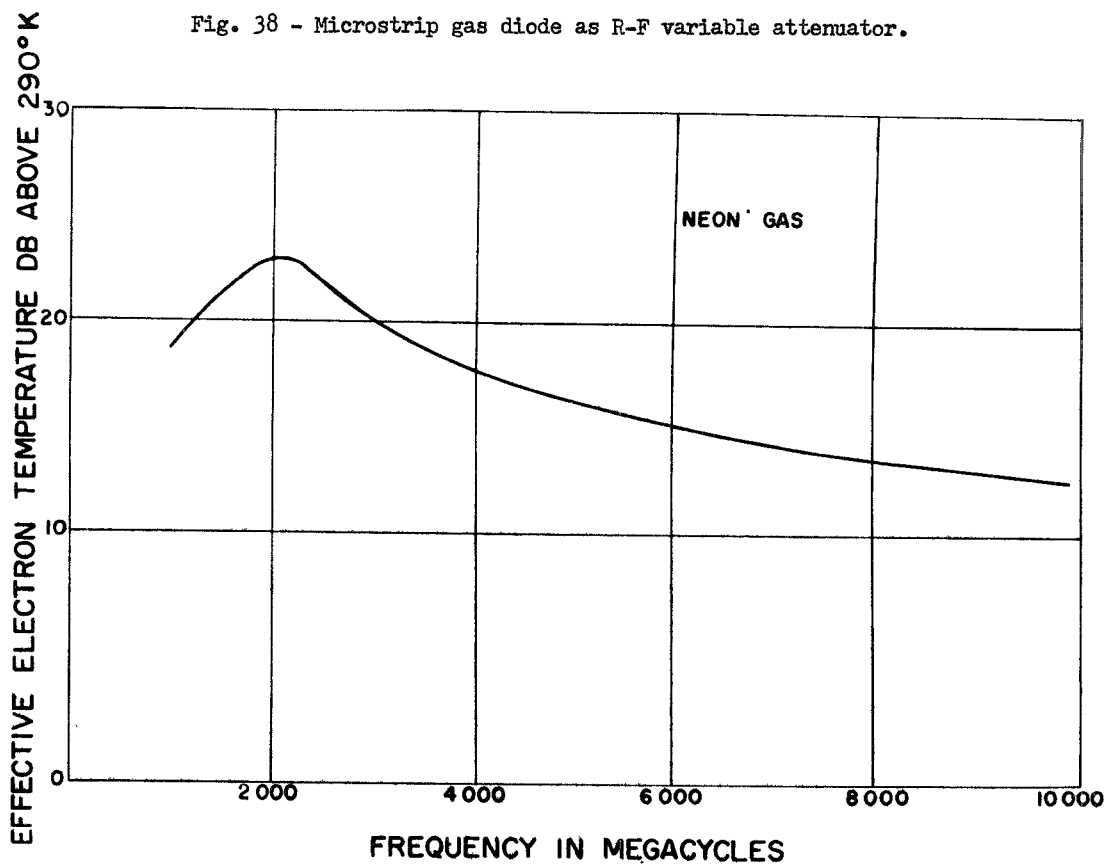


Fig. 39 - Microstrip gas diode used as wide band noise source.

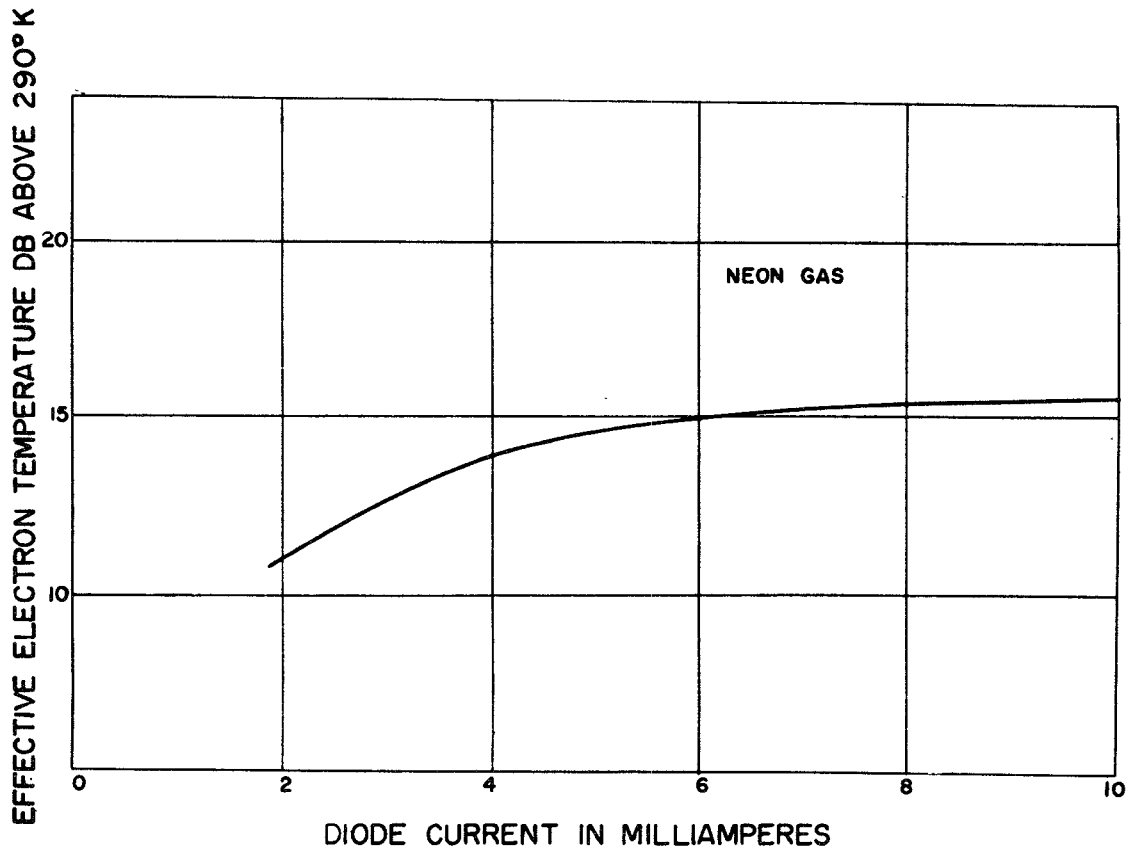


Fig. 40 - Microstrip gas diode used as R-F noise source.

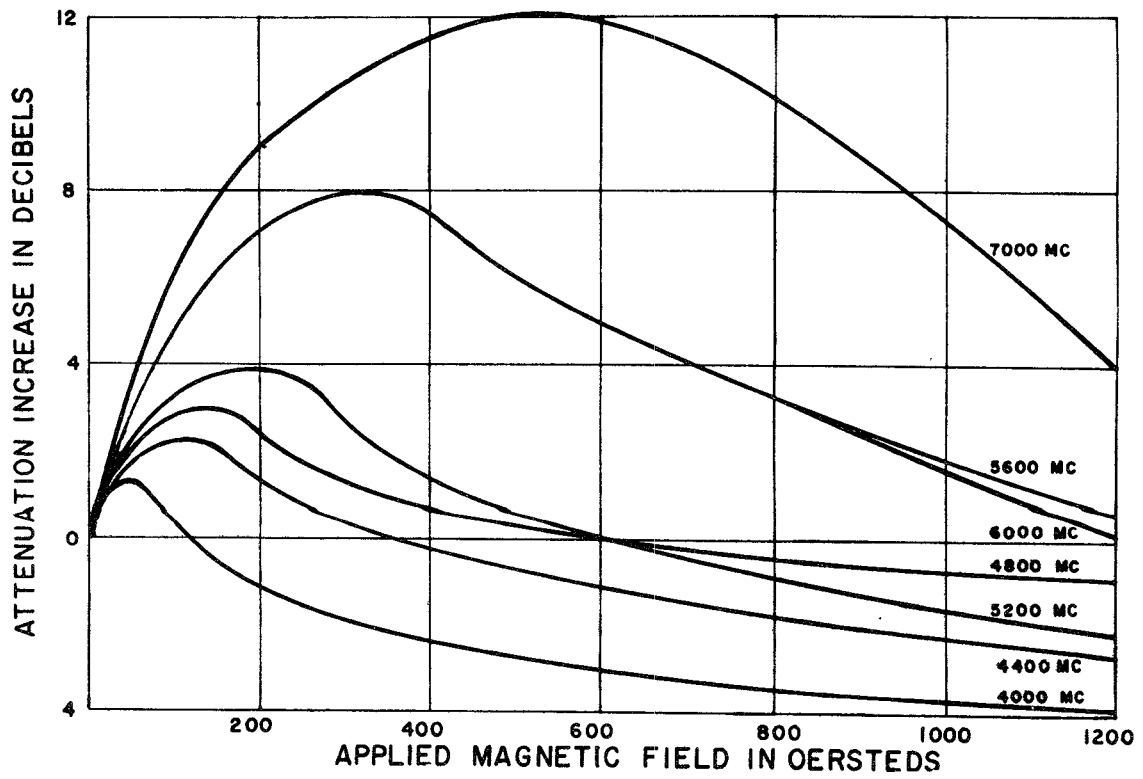


Fig. 41 - Microstrip ferrite R-F attenuation.



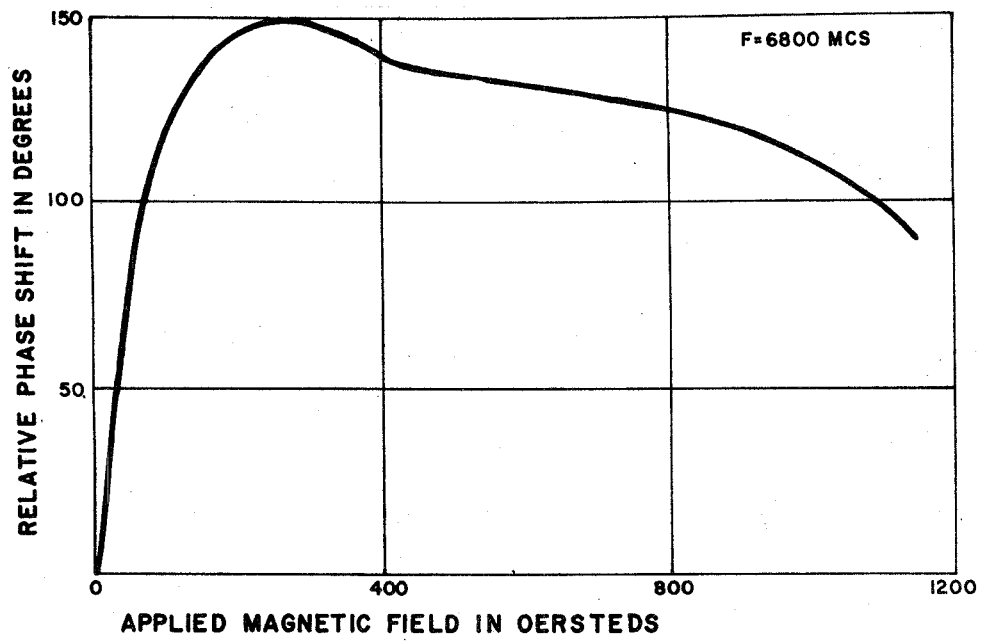


Fig. 42 - Microstrip ferrite phase-shift.

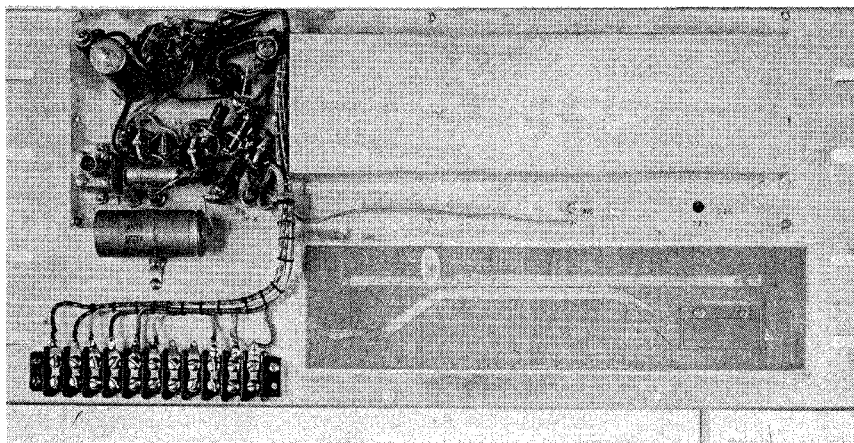


Fig. 43 - Microstrip R-F head for 2000 mc receiver.

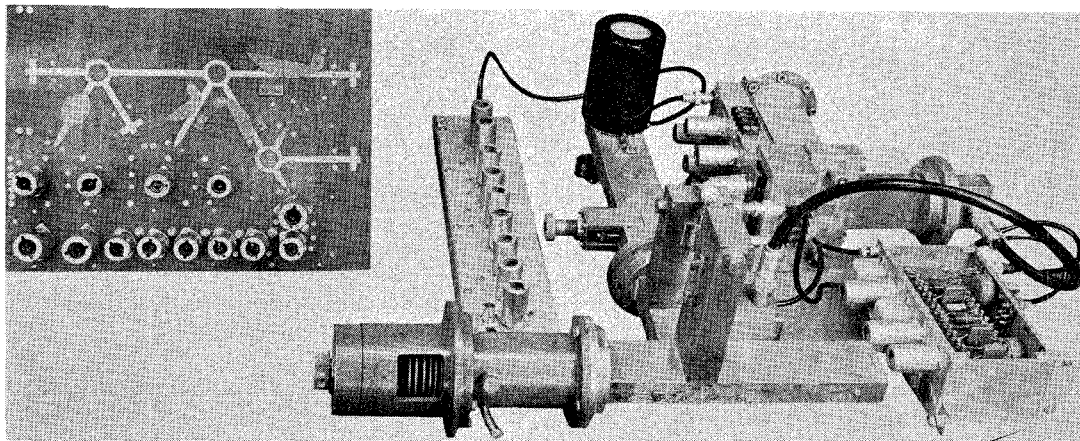


Fig. 44 - Conventional waveguide and microstrip receivers (4400 to 5000 mc).

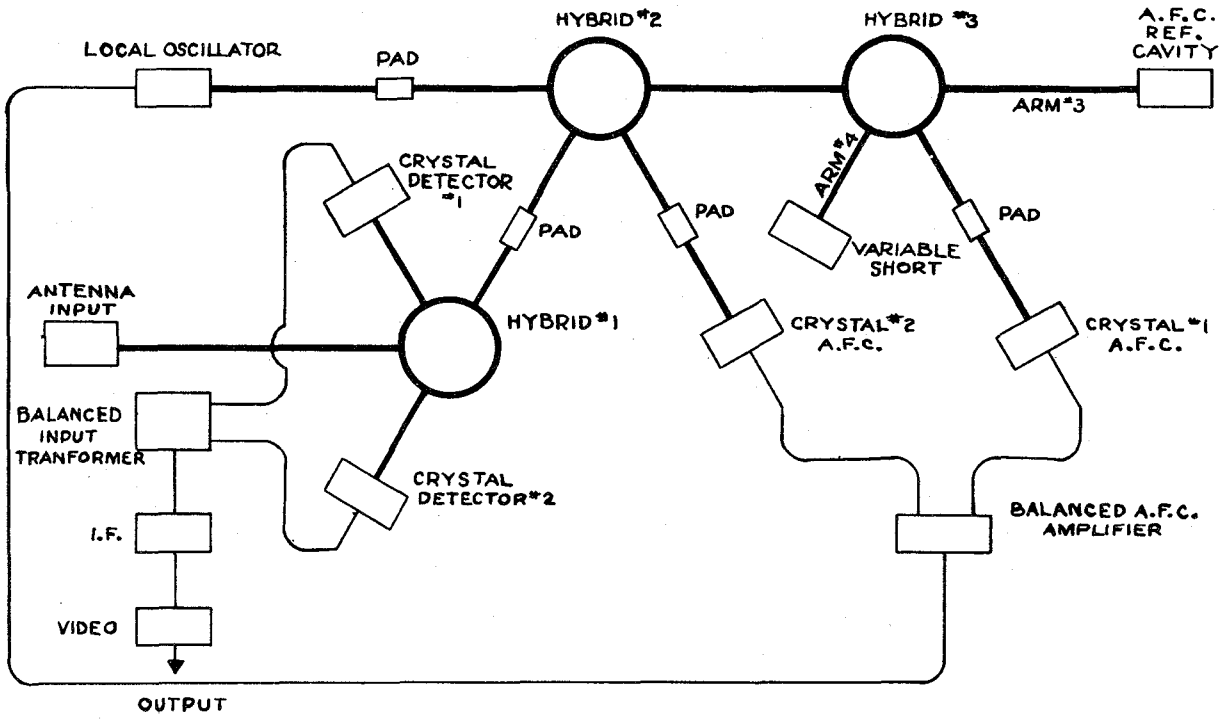


Fig. 45 - Block diagram of the complete microstrip receiver.

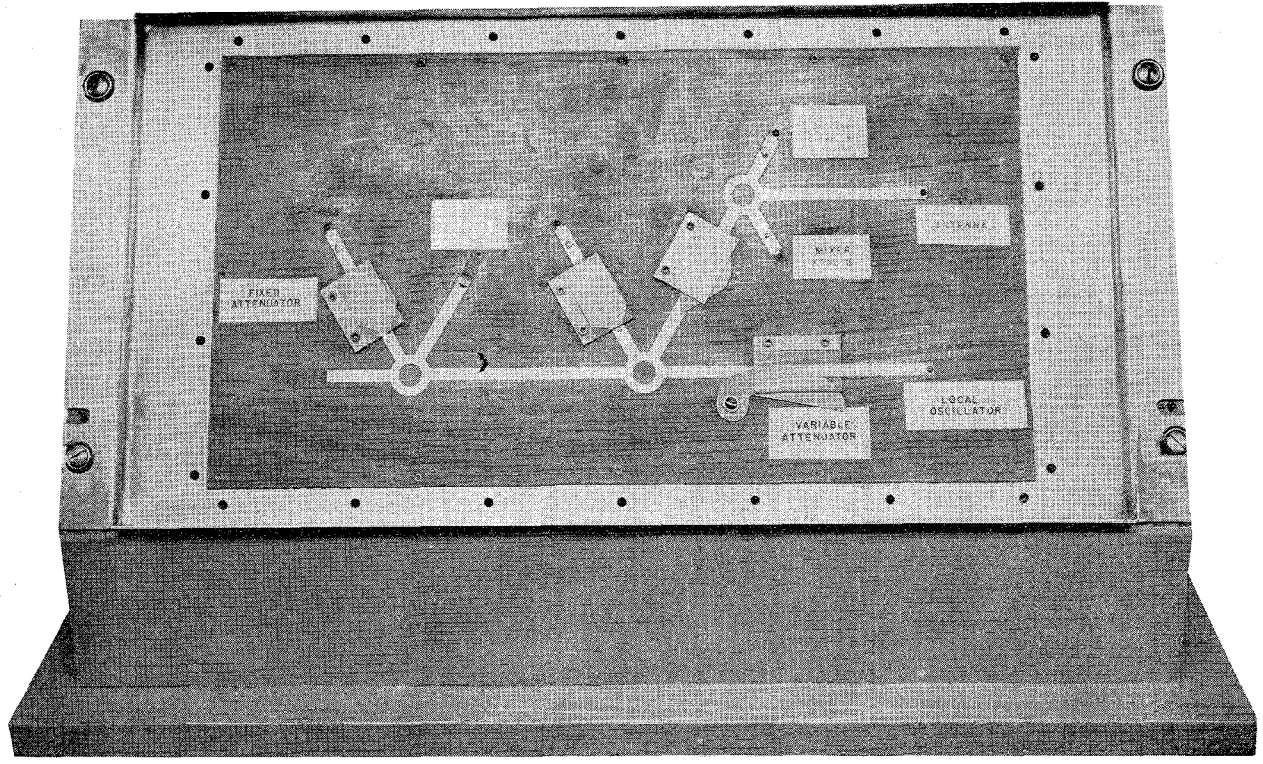


Fig. 46 - Microstrip receiver at 6000 mc - front view.

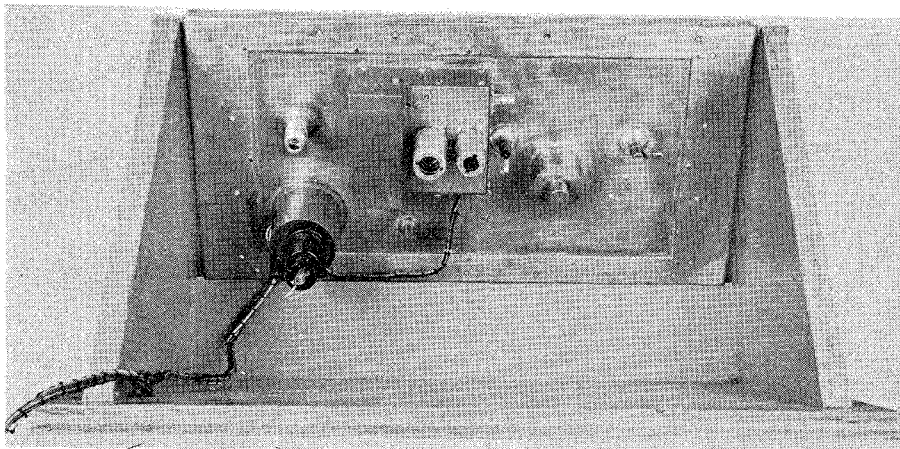


Fig. 47 - Microstrip receiver at 6000 mc - back view.

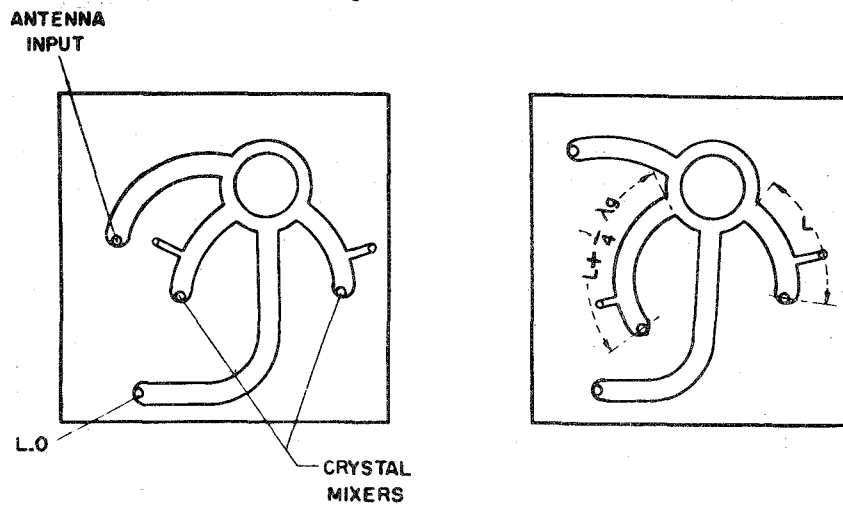


Fig. 48 - Microstrip balanced crystal mixers.

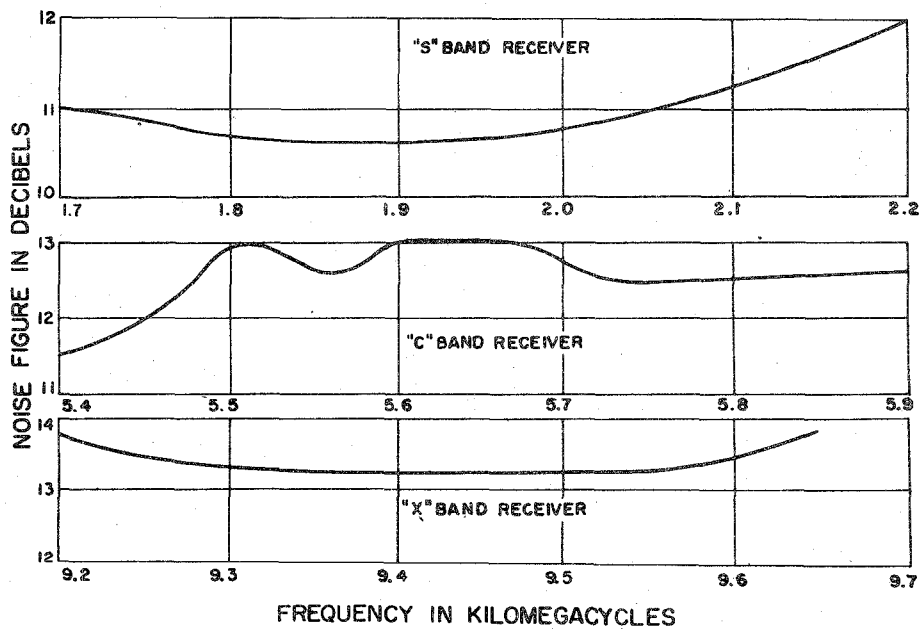


Fig. 49.- Noise figure of microstrip receivers.

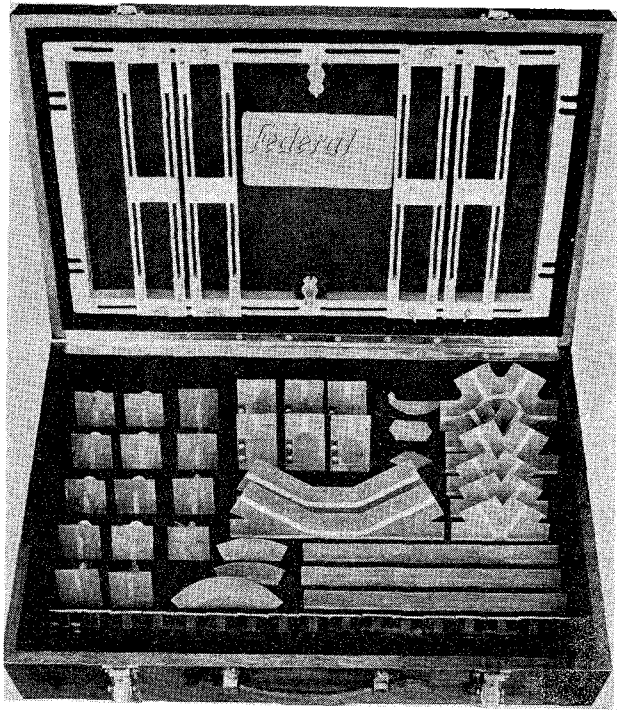


Fig. 50 - Microstrip kit.

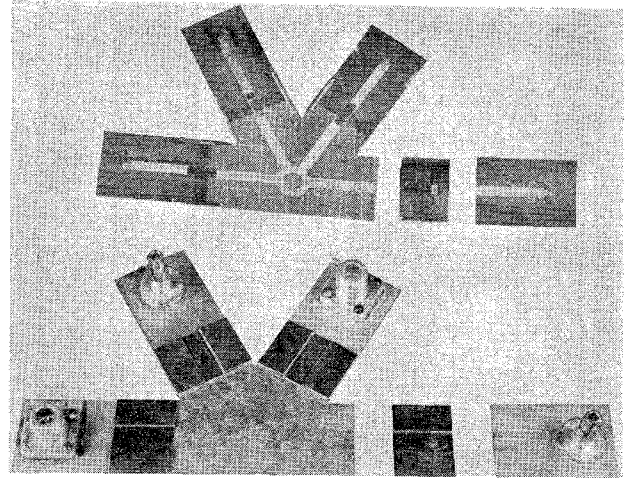


Fig. 51 - Microstrip kit components.

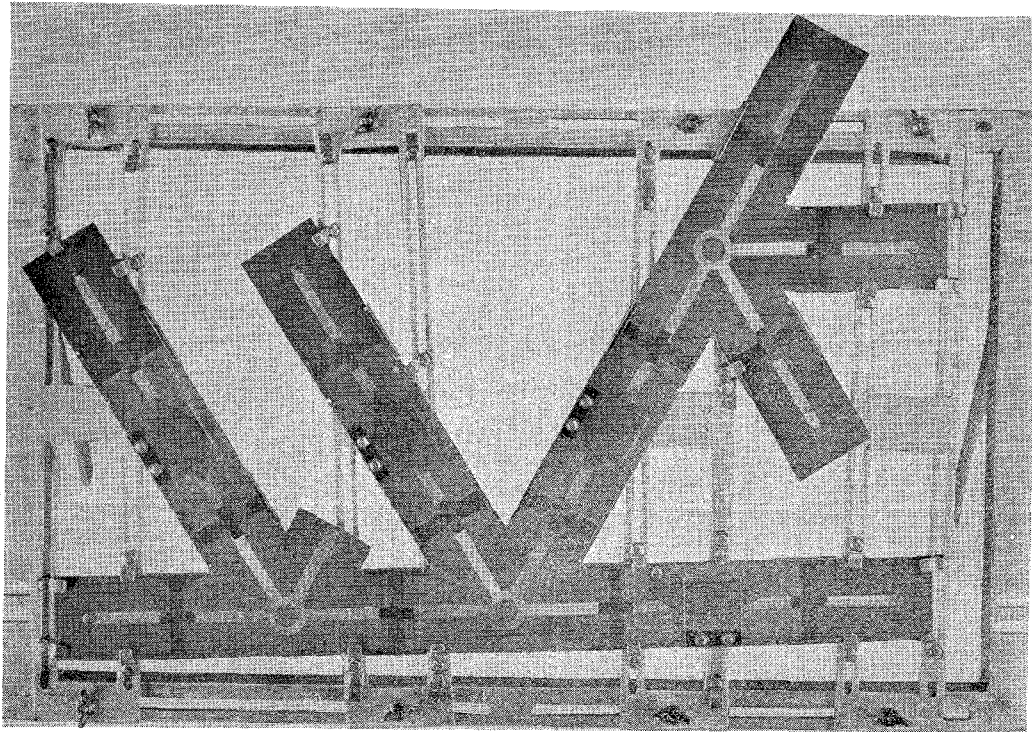


Fig. 52 - Microstrip kit assembly.